





Comparative Biochemistry and Physiology Part B: Biochemistry and Molecular Biology

Volume 257, January 2022, 110678

De novo transcriptome assemblies of red king crab (*Paralithodes camtschaticus*) and snow crab (*Chionoecetes opilio*) molting gland and eyestalk ganglia - Temperature effects on expression of molting and growth regulatory genes in adult red king crab

Øivind Andersen^{a b}  , Hanne Johnsen^{a c 1}, Astrid C. Wittmann^{d e 1}, Lars Harms^e, Tina Thesslund^a, Ragnhild Stenberg Berg^a, Sten Siikavuopio^a, Donald L. Mykles^{f g}

Show more 

 Outline |  Share  Cite

<https://doi.org/10.1016/j.cbpb.2021.110678> 

[Get rights and content](#) 

Under a Creative Commons [license](#) 

open access

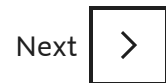
Highlights

- *De novo* transcriptome assemblies made from red king crab and snow crab.
- First description of the ecdysteroid biosynthetic enzymes in anomuran crabs.
- Red king crab has Shade-like enzyme, not Shed possessed by other decapods.

- Key regulatory genes in adult red king crab moderately influenced by temperature.

Abstract

Red king crab (*Paralithodes camtschaticus*) and snow crab (*Chionoecetes opilio*) are deep-sea crustaceans widely distributed in the North Pacific and Northwest Atlantic Oceans. These giant predators have invaded the Barents Sea over the past decades, and climate-driven temperature changes may influence their distribution and abundance in the sub-Arctic region. Molting and growth in crustaceans are strongly affected by temperature, but the underlying molecular mechanisms are little known, particularly in cold-water species. Here, we describe multiple regulatory factors in the two high-latitude crabs by developing *de novo* transcriptomes from the molting gland (Y-organ or YO) and eye stalk ganglia (ESG), in addition to the hepatopancreas and claw muscle of red king crab. The Halloween genes encoding the ecdysteroidogenic enzymes were expressed in YO, and the ESG contained multiple neuropeptides, including molt-inhibiting hormone (MIH), crustacean hyperglycemic hormone (CHH), and ion-transport peptide (ITP). Both crabs expressed a diversity of growth-related factors, such as mTOR, AKT, Rheb and AMPK α , and stress-responsive factors, including multiple heat shock proteins (HSPs). Temperature effects on the expression of key regulatory genes were quantified by qPCR in adult red king crab males kept at 4°C or 10°C for two weeks during intermolt. The Halloween genes tended to be upregulated in YO at high temperature, while the ecdysteroid receptor and several growth regulators showed tissue-specific responses to elevated temperature. Constitutive and heat-inducible HSPs were expressed in an inverse temperature-dependent manner, suggesting that adult red king crabs can acclimate to increased water temperatures.



Keywords

Halloween genes; Anomura; Y-organ; Ecdysteroids; Thermal acclimation

1. Introduction

Red king crab and snow crab are giant deep-sea predators in the benthic ecosystems of sub-Arctic regions in the North Pacific and North Atlantic Oceans. Red king crab is among the world's largest arthropods attaining weights up to 11 kg and with legs spanning 1.8 m, while snow crab is slightly smaller (Stevens, 2014). They are highly important commercial fisheries resources, and both species have established non-native populations in the Barents Sea. Snow crabs inhabit depths down to 1400 m at temperatures from -1.5°C to 4°C year-round (Squires, 1990; Dawe and Colbourne, 2002), while red king crabs occur at depths down to 400 m in the Barents Sea with temperatures ranging from below freezing to about 8°C (Stiansen et al., 2009). Adult snow and king crabs showed behavioral thermoregulation in laboratory experiments by selecting the coldest end ($1.5\text{--}3.5^{\circ}\text{C}$) of the temperature gradient (Christiansen et al., 2015; Siikavuopio et al., 2019). Increased abundance and spread of the two invasive crab species may have great impact on the native life in the sub-Arctic region in the future (Jørgensen and Primicerio, 2007; Oug et al., 2011; Falk-Petersen et al., 2011). Changes in abundance and biodiversity relate to temperature changes and variability, as well as to predation and fishing pressure (Dvoretzky and Dvoretzky, 2016; Dvoretzky and Dvoretzky, 2020; Green et al., 2014; Poloczanska et al., 2016; Quinn, 2017; Scheffers et al., 2016). Ectotherms will only grow in the thermal range in which energy supply from aerobic metabolism is higher than the maintenance costs (Pörtner and Knust, 2007; Pörtner, 2010; Sokolova et al., 2012). The energy budget in snow crab seems to become negative above 7°C due to reduced feeding and rising metabolic costs, and adult red king crab males kept at 4°C , 8°C or 12°C for 110 days showed higher food conversion efficiency at the lowest temperature and higher mortality at elevated temperatures (Foyle et al., 1989; Thompson and Hawryluk, 1990; Siikavuopio et al., 2017). Temperature is a major external factor influencing physiological rates, growth and molting in crustaceans (Hartnoll, 1982, Hartnoll, 2001; Anger et al., 2003; Wittmann et al., 2011, Wittmann et al., 2012, Wittmann et al., 2018). Juvenile red king crabs showed increased growth up to 15°C and an inverse exponential relationship between intermolt period and temperature up to 12°C (Stoner et al., 2010; Long and Daly, 2017). Similarly, intermolt period was shorter at 8°C than at 3°C in juvenile snow crabs (Yamamoto et al., 2015).

The cyclic shedding of the chitinous exoskeleton is essential for growth and development in crustaceans. Molting is regulated by complex interactions between conserved neuropeptides produced in the eyestalk ganglia (ESG) and molting hormones (ecdysteroids) secreted from the paired molting glands, or Y-organs (YO), situated in the anterior cephalothorax (Mykles, 2011; Mykles and Chang, 2020). During intermolt, the synthesis and secretion of ecdysteroids are inhibited by the pulsatile release of molt-inhibiting hormone (MIH) and crustacean hyperglycemic hormone (CHH) from the X-organ-sinus gland complex in the ESG, while the reduced levels of circulating MIH at early premolt induces

hypertrophy of YO and activates ecdysteroid synthesis (Mykles and Chang, 2020). The pleiotropic CHH exerts an inhibitory effect on molting and reproduction, but also plays a role in the acute response to environmental stressors (Webster, 1996; Lorenzon et al., 2004; Fanjul-Moles, 2006). Dietary cholesterol is converted to ecdysteroids through a series of catalytic reactions involving the Rieske-oxygenase Neverland (Nvd) and five cytochrome P450 (CYP450) monooxygenases encoded by the Halloween genes *spook* (CYP307A1), *phantom* (CYP306A1), *disembodied* (CYP302A1), *shadow* (CYP315A1), and *shade* (CYP314A1) or *shed* (CYP314A1) (Mykles, 2011; Goody et al., 2014; Qu et al., 2015; Ventura et al., 2017; Swall et al., 2021). The upregulated ecdysteroid synthesis at premolt is associated with increased expression of the ecdysteroid receptor (EcR), which forms a functional heterodimer with the retinoid x receptor (RXR) (Yao et al., 1993; Chung et al., 1998).

Tissue growth is regulated by the highly conserved mechanistic Target of Rapamycin (mTOR) controlling protein synthesis and gene expression in response to nutrients, growth factors, and stressors (Saxton and Sabatini, 2017; Liu and Sabatini, 2020). mTOR activity is required for ecdysteroidogenesis and up-regulates ecdysteroid biosynthetic genes in the YO (Mykles and Chang, 2020; Shyamal et al., 2018). An activating key regulator of mTOR is Ras homolog enriched in brain (Rheb), and molting increases *Rheb* mRNA levels in the YO (Das et al., 2018; Shyamal et al., 2018; Wittmann et al., 2018). Rheb is controlled by the inhibitory tuberous sclerosis complex (TSC1/2), which in turn is inhibited by AKT (also known as protein kinase B) and activated by AMP kinase (AMPK) (Saxton and Sabatini, 2017; Liu and Sabatini, 2020).

Red king crab and snow crab belong to the suborders Anomura (“half” crabs) and Brachyura (“true” crabs), respectively, which diverged about 325 million years ago (Wolfe et al., 2019). These crabs are excellent models for understanding how climate change and associated water temperature changes may influence important physiological processes in cold-water crustaceans. The planktonic larvae of red king crab tolerate a wide range of temperatures, and larvae acclimated to 14°C displayed higher tolerance to warm challenge temperatures compared to those reared at 4°C or 8°C (Michelsen et al., 2019). Juvenile red king crabs showed strong compensatory shifts in gene expression in response to acclimation to 10.5°C, 12.5°C or 14.5°C in a transcriptome-wide whole organism study (Stillman et al., 2020). Similar growth in adult red king crabs kept at 4°C, 8°C or 12°C (Siikavuopio and James, 2015) suggests that adults are also capable to acclimate to a wide range of temperatures, but the underlying compensatory mechanisms on tissue level are unknown. Genomic resources from the two species have recently become available in studies of transcriptomic response to seismic surveying noise in snow crab hepatopancreas (Hall et al., 2020) and to decreased pH and elevated temperature in whole pre-adults and in heart, gill and integument of adult

red king crabs (Stillman et al., 2020). Here, we generated *de novo* transcriptome assemblies from the YO and ESG in both species and from hepatopancreas and claw muscle in red king crab. Multiple regulatory, molt-related, and endocrine factors were for the first time described in the two crab species. Expression of mTOR signaling, Halloween, *EcR* and *hsp* genes were measured by real-time quantitative polymerase chain reaction (qPCR) in YO, ESG, hepatopancreas and claw muscle of male red king crabs in intermolt kept at 4°C or 10°C for 14 days to study how a cold-water crab copes with exposure to elevated temperature.

2. Materials and methods

2.1. Animals

Adult red king crabs were caught by local fishermen in the sea off Varangerfjorden in Finnmark county, Norway and transported to the Aquaculture research station at Kårvika Research Station, Tromsø, Norway in January 2018. The crabs were held in two 3 m² (900l) tanks each divided into four 0.75 m² compartments with their own water inlet at ambient temperature (2.5–4.0°C) under natural light and photoperiod. Adult male snow crabs were caught in the Bering Sea late autumn 2017 and transported to the Station where they were kept in round tanks (1.75 m²) with shaded natural light and a water temperature ranging between 2.0 and 3.8°C. Both species were fed in excess with pollock, herring and blue mussel three times weekly. Before sample collection, crabs were anaesthetized with clove oil (0.125 ml/l seawater, NOW Foods, USA) and sacrificed by an incision of the supraesophageal ganglion (brain).

For generating transcriptome assemblies, YO and ESG were collected from one snow crab in intermolt stage at 10. Feb. 2018 and stored in RNAlater (Ambion, 1:10 volume ratio) at –20°C after 4°C overnight. Putative YO, ESG, hepatopancreas and major claw muscle were dissected from two male red king crabs in early and late premolt stages at 21. Feb. and 13. March 2018, respectively. Several putative YO-containing tissues were collected and bisected with one part fixed in 10% formalin (Kemetyl) and the other submerged in RNAlater, which was also used for securing the other tissue samples.

For the temperature experiment, a total of 56 male red king crabs in postmolt were acclimated to 4°C for 11 weeks in the two tanks described above. It should be noted that the water supply to both tanks was accidentally disturbed for a few hours six days before the first sampling (T0) that caused a temperature drop. At 25. April 2018 eight crabs were collected from both tanks and sacrificed before samples were secured as described above. The water

temperature in one of the tanks was then kept at 4°C, while the other tank was raised to 10°C by increasing the temperature with 1 degree per day. After 14 days at 4°C or 10°C, eight crabs were sacrificed and samples were dissected at 15. May 2018 (T1).

2.2. Molt-staging

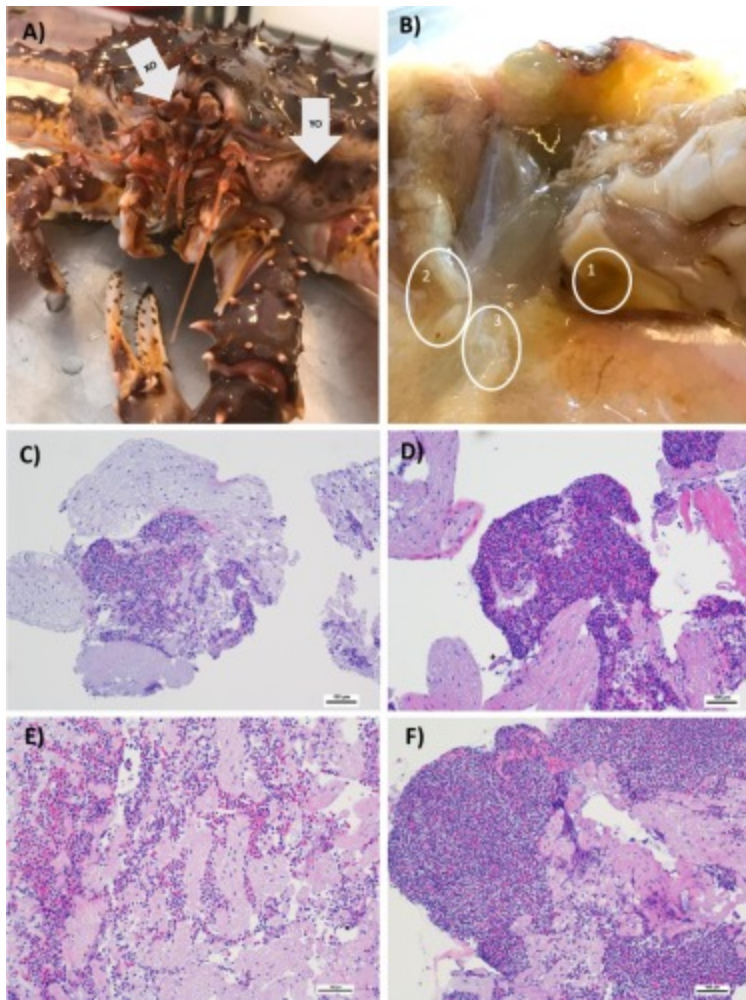
Molt cycle stages were determined by inspection of the cuticle thickness and setal development of scaphognathites ([Moriyasu and Mallet, 1986](#)). They were dissected and submerged in crab saline (430mM NaCl, 5mM K₂SO₄, 7mM MgCl₂, 4.5mM, CaCl₂, and 10mM HEPES–NaOH; pH7.2, [Lee et al., 2007](#)) and kept at 4°C for at least 24h before analysis using light microscopy (Nikon Eclipse Ci) and the Nikon Nis-Elements Basic Research software.

2.3. Histology

Formalin-fixed putative YO tissues were processed overnight in Tissue Processor (Logos, Milestone). Paraffin embedded tissues were sectioned (2µm) using a rotary microtome (Leica) and stained with hematoxylin and eosin (Merck) in auto-stainer (Leica) at the Norwegian Veterinary Institute, Harstad. All slides were then analyzed at Nofima, Tromsø, using light microscopy (Nikon Eclipse Ci) and the Nikon Nis-Elements Basic Research software. Candidate YO specific cells were verified by transcriptome analysis of parallel samples stored in RNAlater.

2.4. RNA extraction and transcriptome analyses

Total RNA was isolated from two putative YO samples (localization see [Fig. 1B](#)), ESG, major claw muscle and hepatopancreas dissected from two red king crabs at early and late premolt stage, and from the YO and ESG of one snow crab in intermolt using AllPrep DNA/RNA/miRNA Universal Kit (Qiagen) according to the manufacturer's protocol. RNA quality and quantity were determined using NanoDrop 8000 (Thermo Scientific) and Bioanalyzer (Agilent). A260/280 and A260/230 ranged from 1.93–2.22 to 0.95–1.96, respectively, while RIN values ranged from 5 to 10. It is known that RNA of arthropods is inclined to appear degraded using Bioanalyzer due to a gap deletion of 28S ribosomal RNA (rRNA) subunit ([McCarthy et al., 2015](#); [DeLeo et al., 2018](#)). Thus, heat-denatured and untreated samples were analyzed using the Bioanalyzer. Ten samples were shipped to the Norwegian Sequencing Centre, Oslo, Norway, for Illumina sequencing. Briefly, libraries were prepared using a Strand-specific TruSeq RNA-seq library prep kit (Illumina), and paired-ends sequenced using a HiSeq 3/4000 Genome Analyser (Illumina), in one lane with a read length of 150bp.



Download: [Download high-res image \(699KB\)](#)

Download: [Download full-size image](#)

Fig. 1. Identification of Y-organ (YO) in red king crab. A) Localization of YO in the fused segments of the mouthparts and of the paired X-organ (XO) in the eyestalks. B) The three areas included in the search for YO. C-F) Histology of glandular tissue in YO. C) KingCrab16_YO2, area #1 sample 2. D) KingCrab16_YO3, area #1 sample 3. E) KingCrab20_YO1, area #1. F) KingCrab20_YO2, area #2. Scale bar 100 μ m. (For interpretation of the references to colour in this figure legend, the reader is referred to the web version of this article.)

Raw reads were quality controlled by FastQC v. 0.11.7 (Babraham Institute, Cambridge, UK). Adapter sequences were removed with bbdutk.sh, from the BBtools suite, version 38.01 ([Bushnell, 2015](#)) with following parameters: ktrim=r, k=23, mink=11, hdist=1, tpe, tbo. Remaining sequences were checked for rRNA sequences by SortMeRNA version 2.1 ([Kopylova et al., 2012](#)) and removed before further processing. To filter the sequences for the common Illumina spikein PhiX, bbdutk.sh was used with a kmer size of 31 and a hdist of 1. A final quality trimming was performed with bbdutk.sh using Q10 as minimum quality and 36

bases as the minimum length. All obtained sequences were normalized using `bbnorm.sh` ([Bushnell, 2015](#)) with an average depth of 200× and a minimum depth of 5× before they were *de novo* assembled using the Trinity genome-independent transcriptome assembler (release 2.6.6; ([Grabherr et al., 2011](#))) with a minimum transcript length of 300 bases and the option for strand specificity set (`--SS_lib_type RF`). For each of the king crabs separate assemblies of claw muscle and putative YO tissues (two samples per animal) were generated ([Table 1](#); KingCrab16_MC, KingCrab16_YO2, KingCrab16_YO3, KingCrab20_MC, KingCrab20_YO1, KingCrab20_YO2. KingCrab16_YO2, KingCrab16_YO3 and KingCrab20_YO1 were sampled from Area #1 and KingCrab20_YO2 was sampled from Area #2, see [Fig. 1B](#)), as well as assemblies that contained all reads from all the tissues of one individual (KingCrab16 and KingCrab20). Furthermore, reads of both individuals were combined to a comprehensive assembly (KingCrab16_20). For the snow crab, one assembly, which contained reads from YO only (SnowCrab9_YOa) and one of YO and ESG combined were generated (SnowCrab9). The read representations of the assemblies were assessed using the Bowtie2 2.3.4.1 software. The completeness was evaluated using the package BUSCO v3.0.0 (Benchmarking Universal Single-Copy Orthologs) and the orthologs of the public database "Arthropoda_odb9 (1066)". The annotation of the *de novo* assembled transcriptomes was performed using the Trinotate functional annotation suite (v 3.1.1; ([Grabherr et al., 2011](#))), including homology searches against the UniProt Swiss-Prot and NCBI non-redundant databases. MEtaGenome ANalyzer (MEGAN Community Edition, version 6.20.17) was used to explore eggNOG and KEGG pathway assignments and test for similarity among tissue-specific assignments of KEGG proteins by generating an UPGMA tree using the Bray-Curtis method.

Table 1. Assembly and annotation results based on all transcript contigs. King crab 16 was in premolt, king crab 20 was in late premolt, snow crab 9 was in intermolt. The assemblies SnowCrab9, KingCrab16 and KingCrab20 used reads from multiple tissue types per individual, the assembly KingCrab16_20 used reads of all available tissues of both animals. KingCrab16_YO2, KingCrab16_YO3 and KingCrab20_YO1 were sampled from area #1, KingCrab20_YO2 was sampled from area #2 (see [Fig. 1B](#)). Note that it is unlikely that putative YO samples of king crab 16 were Y-organ tissue due to the absence of Halloween genes (see [Supplementary Table S1](#)). NR: NCBI non-redundant, SP: UniProt/Swiss-Prot databases, eggNOG: nested orthologous gene groups, KEGG: Kyoto Encyclopedia of Genes and Genomes, GO: Gene Ontology, MC: claw muscle, YO: Y-organ, ESG: eyestalk ganglia, HP: hepatopancreas.

Assembly	Tissue types	Total number of genes	Total number of transcripts	Median length (N ₅₀) of transcripts (bp)	Mean length (bp)	Total number of assembled bases	Overall alignment rate (%)	Number of hits (genes)
KingCrab16_MC	MC	40,941	56,911	1387	989	56,302,748	94.25	935
KingCrab16_YO2	unknown	55,435	78,090	1015	832	64,957,394	90.21	11,7
Area #1, sample 2								
KingCrab16_YO3	unknown	58,899	82,295	1166	898	73,888,198	91.31	11,9
Area #1, sample 3								
KingCrab20_MC	MC	39,106	53,921	1306	955	51,510,966	92.50	890
KingCrab20_YO1	YO	77,081	111,353	1327	960	106,925,376	89.94	15,1
Area #1								
KingCrab20_YO2	YO	76,992	111,341	1312	956	106,417,770	90.12	15,0
Area #2								
SnowCrab9_YOa	YO	57,079	97,557	1507	1015	99,003,920	89.05	16,1
SnowCrab9	YO, ESG	77,726	136,190	1491	1005	136,827,018	91.35	23,4
KingCrab16	YO2, YO3, (i.e. unknown) ESG, HP, MC	150,154	226,560	1267	908	205,705,100	92.05	23,0
KingCrab20	YO1, YO2, ESG, HP, MC	144,844	222,726	1407	962	214,241,763	91.94	13,5
KingCrab16_20	YO, ESG, HP, MC	195,879	305,476	1278	904	276,268,985	91.65	27,5

Halloween gene transcripts in the king crab and snow crab assemblies were identified by a local blastn against *Gecarcinus lateralis* sequences (Benrabaa, 2019; Swall et al., 2021; Supplementary Table S2). Once available, text searches within the annotation results were done to identify assembled sequences of Halloween genes and other genes of interest for qPCR and construction of phylogenetic trees.

Multiple peptide sequences were imported to MEGA X (Kumar et al., 2018) and aligned using MUSCLE (Edgar, 2004). The analyses were conducted using the Maximum Likelihood method. The best model for each alignment was chosen using the ML option (Find the best DNA/protein models) provided by the software. Models with the lowest BIC scores (Bayesian Information Criterion) are considered to describe the substitution pattern the best. Based on the BIC values the LG (+G+I) model (Le and Gascuel, 2008) was chosen for the Halloween genes, while the JTT (+G) model (Jones et al., 1992) was chosen for the CHH, MIH, ITP and ITP-like genes. For both trees a discrete Gamma (+G) distribution was used to model evolutionary rate differences among sites. For the Halloween genes, the rate variation model allowed for some sites to be evolutionarily invariable ([+I], 0.50% sites). The topology with superior log likelihood values were selected. Both the raw reads and the assemblies were deposited in the European Nucleotide Archive (ENA) under study accession number PRJEB44537.

2.5. Quantitative PCR (qPCR) analysis

qPCR was used to measure relative expression of regulatory genes involved in molting, growth and heat response in red king crabs kept at 4°C or 10°C as described in Section 2.1. Total RNA was extracted from the YO, ESG, claw muscle and hepatopancreas of the total of 24 crabs as described in Section 2.4. DNase treatment was performed using the TURBO DNase kit (Ambion) according to manufacturer's protocol. RNA quality and quantity were determined using NanoDrop 8000 (Thermo Scientific). 20µl cDNA was synthesized using the High-Capacity RNA-to-cDNA kit (Thermo Fisher) according to manufacturer's protocol using 200ng input of total RNA. Specific primers were designed using Primer Express 3 software (Life Technologies) for amplification of 17 target genes and 3 reference genes chosen from the generated transcriptomes (Supplementary Table S3). As reference genes we used the housekeeping genes β 1 tubulin, elongation factor 2 (EF2), and ribosomal protein S5 (RPS5) (Fang et al., 2018; Jeon et al., 2020). The geometric mean of the three reference genes showed stable expression levels in the four tissues examined in both temperature groups. The amplification efficiency of each primer pair was calculated using eight 2-fold serial dilutions of a cDNA mix from all four organs according to the equation: $E = 10^{-1/\text{slope}}$ (Pfaffl, 2001). All primer pairs gave single distinctive melting peaks demonstrating that no

primer dimers and unspecific amplification products were present. Absence of genomic DNA was verified by conducted qPCR in the absence of reverse transcriptase on three randomly selected RNA samples, and positive controls contained a cDNA mix from the four tissues. The qPCR was run in duplicates in 384 well plates using QuantStudio 5 (Thermo Fisher) using the following recommended parameters: Standard Run mode with 40 cycles at 50°C for 2min, 95°C for 10min and 60°C for 1 min. Following by the melt curve stage at 95°C for 15s, 60°C for 1 min and 95°C for 15s. Ct threshold was set at 0.1. Each well contained Power SYBR Green PCR Master Mix, 300nM final concentration of each primer, 7µl diluted cDNA (1:40) and nuclease free water (Ambion) to a final reaction volume of 20µl. All data were collected by the Quant Studio Design & Analysis Software (Thermo Fisher) and exported to Microsoft Excel for further analyses. The Pfaffl method was used to calculate relative expression (Pfaffl, 2001), and the geometric mean of the three reference genes was used to normalize the gene expression and remove non-biological variation (Vandesompele et al., 2002). Values from groups with lowest expression was used as calibrator as denoted by Pfaffl (2001).

2.6. Statistical analyses

Statistical analysis of gene expression was conducted in Microsoft Excel. Comparison between groups were performed using the unpaired Student's *t*-test. Values of $p < 0.05$ were considered significant.

3. Results

3.1. Identification of Y-organ

The YO of red king crab was localized ventrally near the basis of the mouth parts below an externally visible brown spot close to the urinary opening (Fig. 1A; see Tudge et al., 2012). The YO is a diffuse, anastomosing gland supported by connective tissue. As it was difficult to visually distinguish the YO from the surrounding tissue, three areas were sampled for histological analysis (Fig. 1B). The YO cells were characterized by high nuclear density that was easily distinguished from the low nuclear density of the surrounding connective tissue in samples taken from Areas 1 and 2, whereas Area 3 did not contain YO tissue (Fig. 1C-F). Consequently, YO tissue from areas #1 and #2 were used from RNA sequencing. In contrast, the YO of snow crab was identified as an ellipsoid, compact white gland clearly distinguishable from the surrounding connective tissue.

3.2. Sequence data and *de novo* transcriptome assemblies

Eleven *de novo* transcriptome assemblies were generated from YO, ESG, hepatopancreas and claw muscle of two individuals of red king crab and from YO and ESG of one snow crab in intermolt ([Table 1](#)). For red king crab, we generated separate assemblies of claw muscle and putative YO tissues, as well as assemblies that contained all reads from all the tissues of one individual. Furthermore, reads of both individuals were combined to a comprehensive assembly. For snow crab, one assembly which contained reads from YO only and one from YO and ESG combined were generated. The total number of assembled bases ranged from 51,510,966 in king crab muscle to 276,268,985 in the comprehensive king crab assembly ([Table 1](#)). The number of Trinity “genes” was in the range 39,106–195,879 and from 53,921 to 305,476 contiguous sequences in total. The mean lengths of the transcripts were in the range 832–1015bp with their median in the range 1015–1507bp. The contig lengths were similar to those obtained in previous studies ([Das and Mykles, 2016](#); [Hall et al., 2020](#)). About 90–94% of the reads mapped back to the transcriptomes using Bowtie. Completeness of Benchmarking Universal Single-Copy Orthologs (BUSCOs) ranged from 64% in the assembly KingCrab16_YO3 to 98% in the comprehensive king crab assembly compared to the Arthropoda_odb9 (1066 BUSCOs) lineage dataset. BLASTx against NCBI non-redundant database and UniProt/Swissprot database resulted in up to 27,536 and 13,360 annotated genes, respectively. 13,320 unique Gene Ontology (GO) terms were identified in the comprehensive king crab assembly, which divide into 1417 terms in the category Cellular Component, 3139 terms in Molecular Function and 8764 terms in Biological Process. Figures tended to be higher than in the study by

[Stillman et al. \(2020, e.g. 18,049 BLASTx hits and 8356 unique GO terms in the Larval transcriptome for comparison\)](#)

, except in contig length, which may be due to different sequencing, assembly and analysis methods. This, too, suggests that genes were represented well, despite focusing on a set of tissue types rather than including whole organisms as in [Stillman et al. \(2020\)](#). When broad eggNOG terms were considered, the number of assignments in muscle and YO tissues were similar ([Fig. 2A](#)). Cluster analysis of KEGG proteins grouped king crab YO and muscle tissue samples, respectively, and identified YO of snow crab as an outgroup ([Fig. 2B](#)).

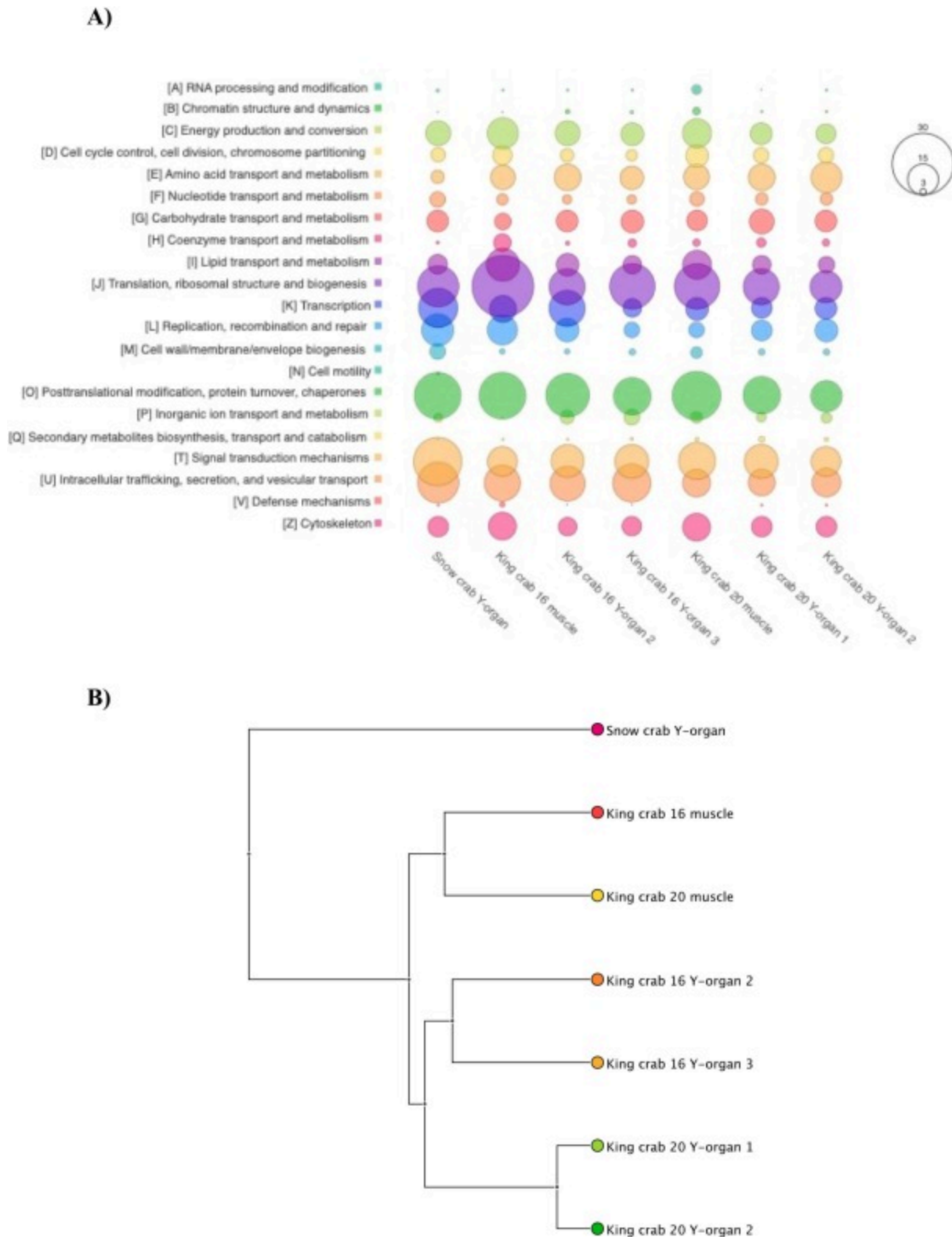


Fig. 2. Comparison of Y-organ and claw muscle annotated transcriptome assemblies of red king crab and snow crab. A) EggNOG contiguous read assignments to the respective categories in snow crab Y-organ and king crab Y-organ and claw muscle. The number of

unclassified contigs is not shown. B) UPGMA tree based on the number of contigs assigned to KEGG terms on enzyme level of samples of snow crab YO, king crab 16 YO2, YO3 and claw muscle and king crab 20 YO1, YO2 and claw muscle using the Bray-Curtis method. Note that it is unlikely that putative YO samples of king crab 16 were Y-organ tissue due to the absence of Halloween genes (Supplementary Table S1). King crab 16 and 20 were in premolt and late premolt, respectively, while snow crab 9 was in intermolt. (For interpretation of the references to colour in this figure legend, the reader is referred to the web version of this article.)

3.3. Identification of multiple molt-, growth- and stress-related factors

The identity of the red king crab YO was confirmed by the identification of the Halloween gene transcripts *spook*, *phantom*, *disembodied*, *shadow* and *shade-like*, together with *neverland* (Supplementary Table S2), which are the first ecdysteroidogenic enzymes described in anomurans. The predicted red king crab enzymes shared high similarity with the brachyuran orthologs, except for Shade-like, which did not cluster with decapod Shed, but branched off from the adjacent Disembodied and non-decapod Shade clades in the phylogenetic tree (Fig. 3). Snow crab YO contained two different *shed* transcripts most similar to *shed4* and *shed5*, in addition to *spook*, *phantom*, *disembodied*, *shadow* and *neverland*. The major ecdysone response gene *Broad-Complex (Br-C)* and the *CYP18A1* gene encoding the enzyme catalyzing 20-HE degradation were also identified in both species.

Several CHH family members, which are characterized by six conserved cysteines, were identified in the red king crab and snow crab transcriptomes. MIH has a glycine residue inserted close to the first cysteine and is lacking a precursor related peptide (PRP) preceding the mature hormone in CHH and non-decapod ITP (Fig. 4A). Red king crab was found to express a single CHH and two highly similar MIH isoforms, in addition to an ion-transport peptide (ITP)-like member. Snow crab ESG contained transcripts encoding single MIH and CHH, which is identical to the recently identified CHH1 isoform (KAG0710697) but showed low similarity with the CHH2 isoform (AHM93480.1, Chung et al., 2014) (Fig. 4A). Red king crab CHH is highly similar to hermit crab CHH (86% identity), but both shared only 56% identity with the squat lobster CHH. Alignment of the three anomurans with the brachyuran mature CHH revealed four positions that distinguish the two groups, but showed conservation of the functionally critical N-terminal dibasic cleavage site, the three disulfide bridges and the C-terminal amidation signal Val-Gly-Lys (Supplementary Fig. S1). The anomuran and brachyuran CHH consistently clustered in the phylogenetic tree, except for snow crab CHH1 (Fig. 4B). Red king crab ITP-like and the brachyuran orthologs formed a clade separate from the insect ITPs and the crustacean MIH clades.

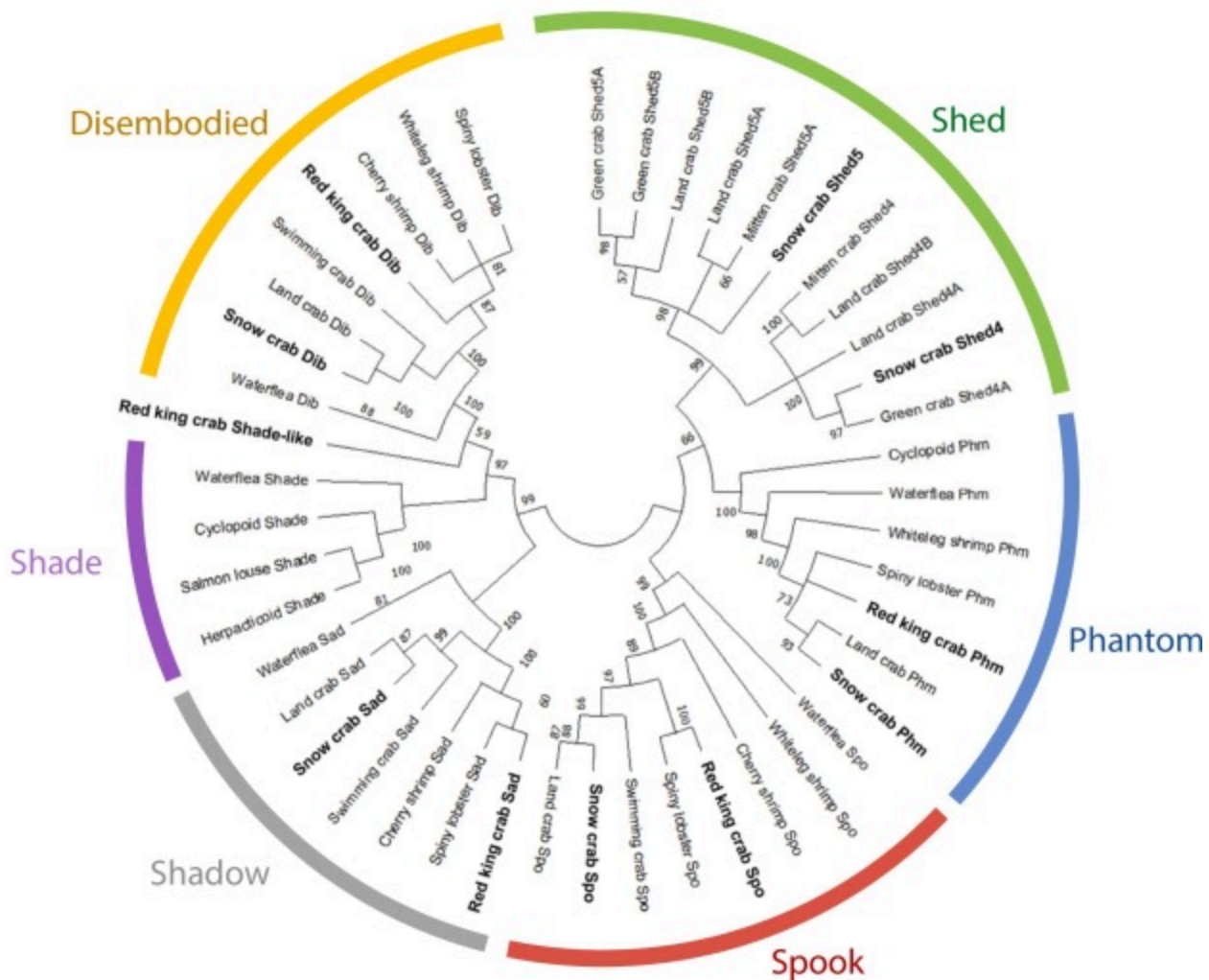
The transcriptomes included a variety of other peptide hormones and neuromodulators, such as red pigment concentrating hormone (RPCH), pigment dispersing hormone (PDH), crustacean cardioactive peptide (CCAP), somatostatin, myostatin, follistatin, allatostatin and cystatin. Growth-related factors in the mTOR signaling pathway comprised mTOR, AMPK α , Rheb, AKT, raptor (regulatory associated protein of mTOR) and rictor (rapamycin-insensitive companion of mTOR) ([Supplementary Table S4](#)).

Both red king and snow crab expressed several molt-related nuclear receptors, including EcR, RXR, E75, HR3 and FTZ-F1 ([Supplementary Table S4](#)). The three EcR isoforms expressed in red king crab are likely coded by two genes designated *EcR1* and *EcR2*, while the alternative splice variant *EcR3* differs from the *EcR1* form in the N-terminal end and in the hinge domain linking the conserved DNA-binding and ligand-binding domains. Various photoreceptors are probably of importance for performing seasonal spawning migrations from large depths to shallow water, and the repertoire of opsins included rhodopsin, melanopsin, peropsin and parapinopsin ([Supplementary Table S4](#)). The crustacean nervous system uses various excitatory and inhibitory neurotransmitters ([Cao et al., 2019](#)) and receptors for glutamate, acetylcholine, histamine, dopamine, GABA and serotonin (5-HT) are expressed in red king crab and snow crab ([Supplementary Table S4](#)).

Among the many stress-response genes expressed by the two crab species, we identified multiple high- and low-molecular HSPs, heat shock factor 1 (HSF-1), hypoxia inducible factor 1 (HIF1) α and β subunits, HIF1 α inhibitor (HIF1AN), HIF-prolyl hydroxylase and hypoxia up-regulated protein 1 (HYOU1). Both species also possessed cold-shock proteins, which are RNA/DNA binding proteins playing a significant role in cold acclimation ([Lindquist and Mertens, 2018](#)) ([Supplementary Table S4](#)).

3.4. Molecular responses of red king crab to elevated temperature

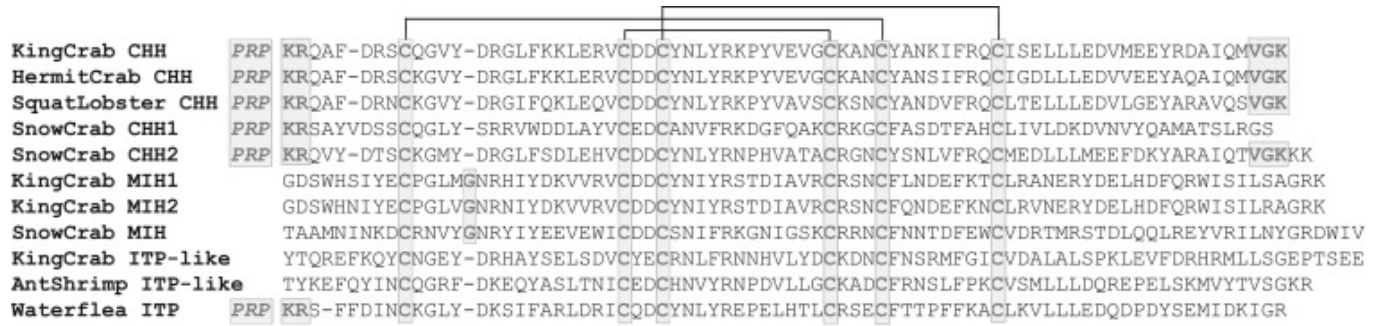
We examined effects of elevated temperature on the expression of key genes involved in molting, growth and heat shock response in male red king crabs kept at either 4°C or 10°C for two weeks. The Halloween genes were mainly expressed in YO and tended to be upregulated at the higher temperature, but significant differences were only found between crabs after 4°C acclimation and after two weeks at 10°C ([Fig. 5A](#)). These groups also differed significantly in the *EcR* mRNA levels in YO with higher levels at 10°C. A similar trend was shown in claw muscle after two weeks at 4°C or 10°C, while the gene expression of the receptor in hepatopancreas were significantly lower at 10°C than at 4°C ([Fig. 5B](#)). The ESG contained about 6-fold higher transcript levels of CHH than MIH, and both tended to be upregulated at high temperature, but the difference was not significant ([Fig. 5C](#)).



[Download: Download high-res image \(417KB\)](#)

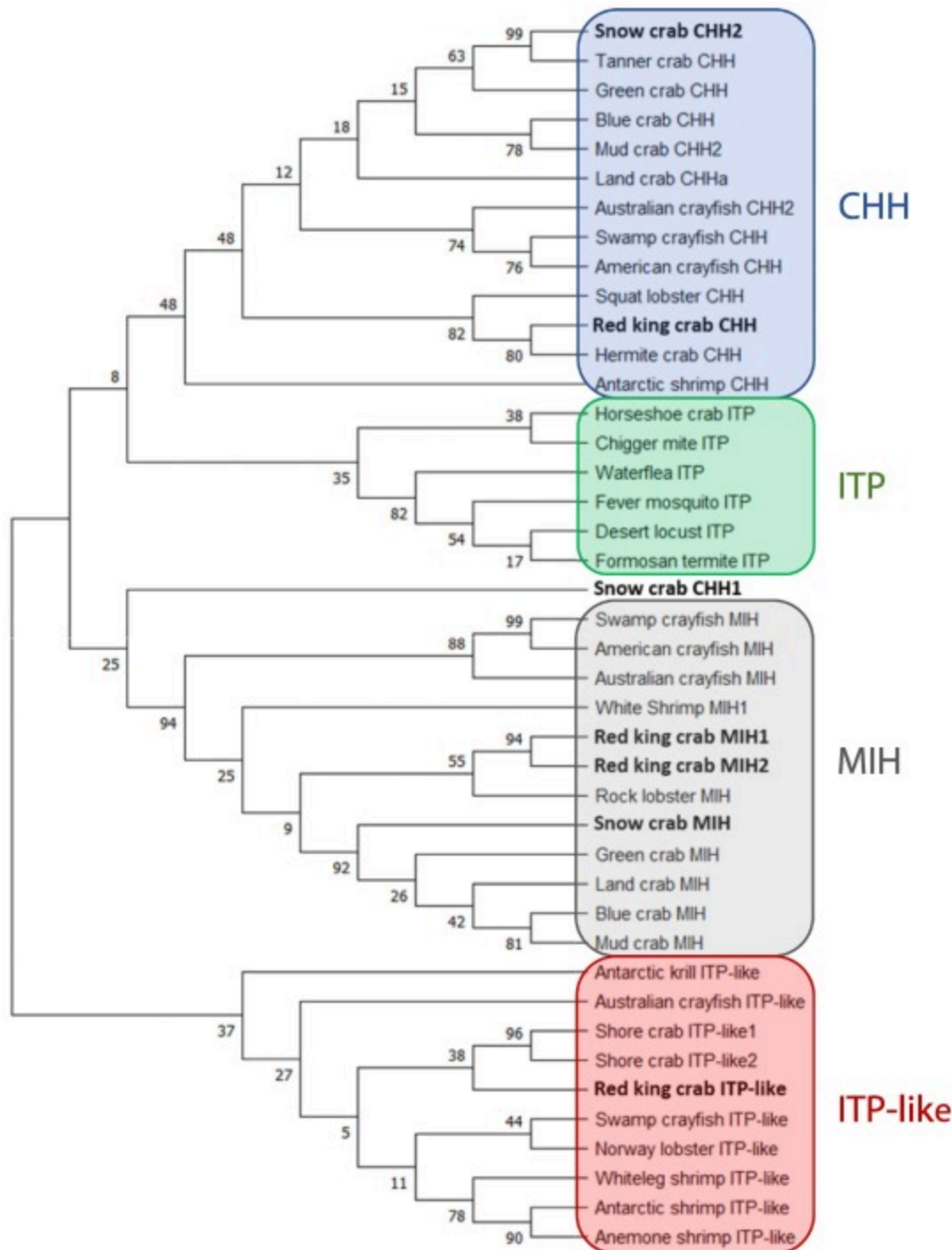
[Download: Download full-size image](#)

Fig. 3. Phylogenetic relationship of the Halloween genes from various crustacean species, including red king crab and snow crab. The tree was generated based on 46 whole amino acid sequences aligned by MUSCLE and there was a total of 698 positions in the final dataset. The analyses were conducted in MegaX using the Maximum likelihood method based on the LG (+G+I) model. To assess the tree topological stability 100 bootstrap resamplings were made. All branches with less than 50 bootstrap confidence value were collapsed. Accession numbers are listed in Supplementary Table S3. (For interpretation of the references to colour in this figure legend, the reader is referred to the web version of this article.)



[Download: Download high-res image \(542KB\)](#)

[Download: Download full-size image](#)

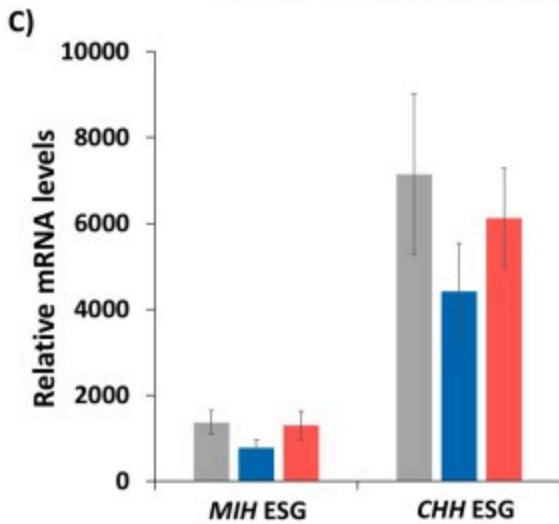
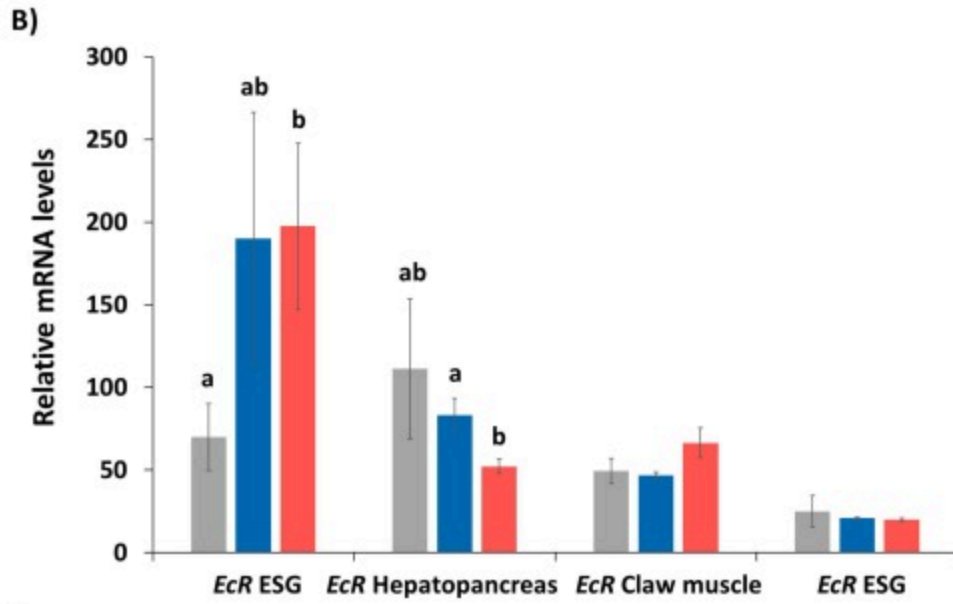
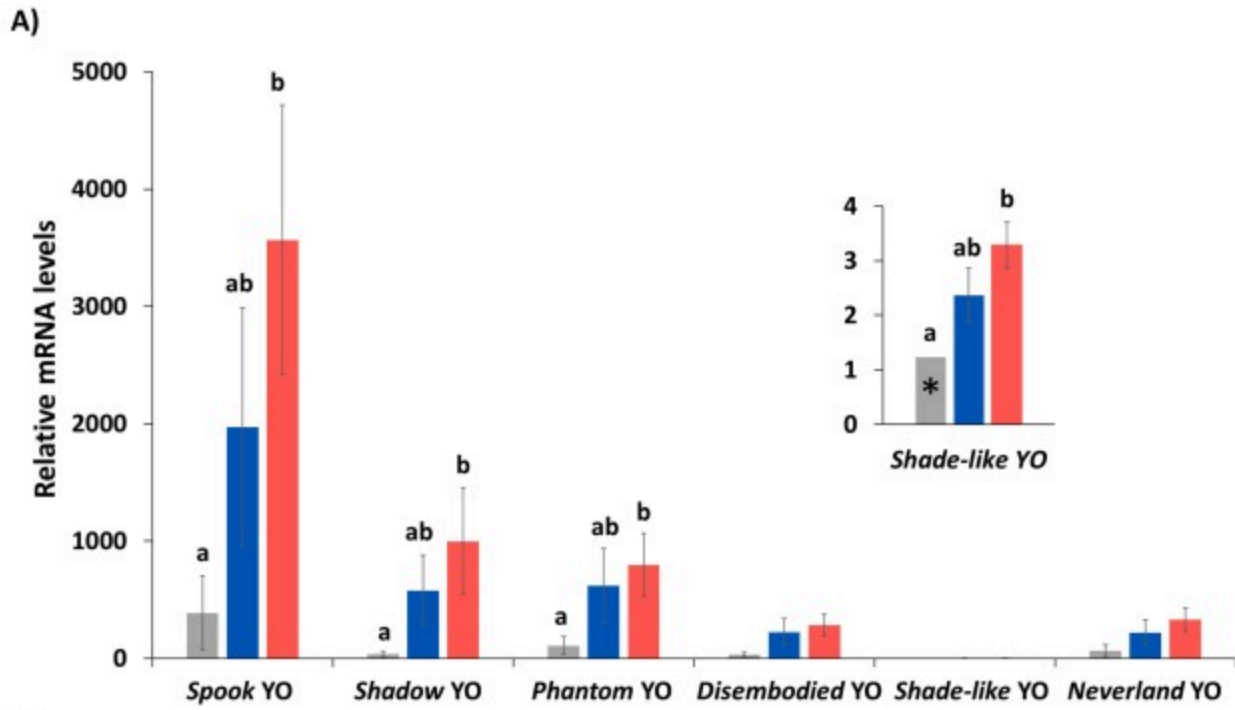


[Download: Download high-res image \(536KB\)](#)

[Download: Download full-size image](#)

Fig. 4. Phylogenetic analysis of CHH family members in red king crab and snow crab. A. Sequence alignment of CHH, MIH and ITP-like from red king crab and snow crab together with hermit crab CHH, squat lobster CHH, Antarctic shrimp ITP-like and waterflea ITP. The six conserved cysteines are colored (yellow), and the PRP region (boxed) and dibasic cleavage site (grey) preceding the mature CHH and ITP are indicated. Predicted C-terminal processing, including putative amide donor Gly (underlined), and the Gly residue (grey) inserted in MIH are also shown. B. Phylogenetic relationship of CHH, MIH, ITP and ITP-like

from various crustaceans, including red king crab and snow crab. The tree was generated based on 42 amino acid sequences aligned by MUSCLE and there was a total of 119 positions in the final dataset. The analyses were conducted in MegaX using the Maximum likelihood method based on the JTT (+G) model. To assess the tree topological stability 100 bootstrap resamplings were made. No branches were collapsed. Accession numbers are listed in Supplementary Table S3. (For interpretation of the references to colour in this figure legend, the reader is referred to the web version of this article.)

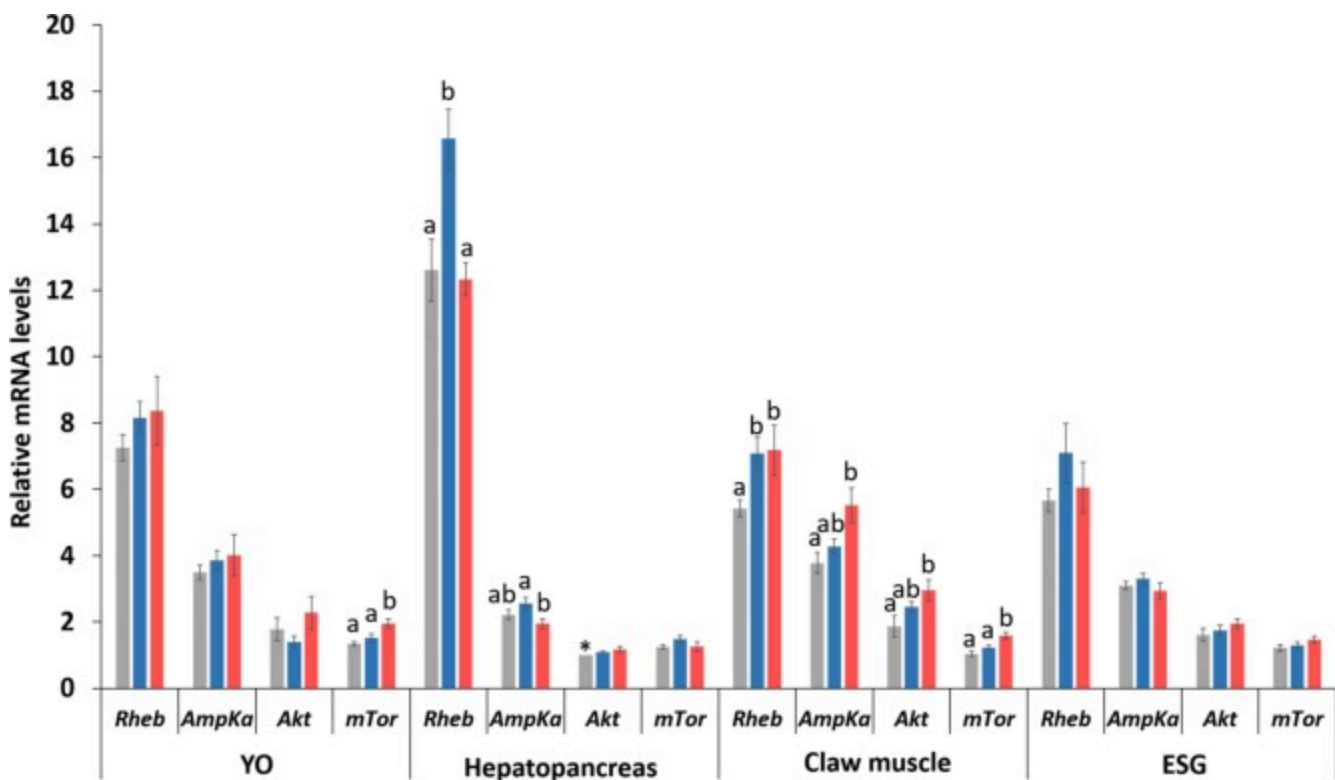


[Download: Download high-res image \(338KB\)](#)

[Download: Download full-size image](#)

Fig. 5. Relative mRNA levels of molt-related genes in adult red king crab measured after 4°C acclimation (grey) and after two additional weeks at 4°C (blue) or 10°C (red) ($n=8$). A) Expression of *spook*, *shadow*, *phantom*, *disembodied*, *shade-like* and *neverland* in YO. B) *Ecdysteroid receptor* (*EcR*) expression in ESG, YO, *hepatopancreas* and claw muscle. C) Expression of *MIH* and *CHH* in ESG. The results were calibrated to the mean expression of *shade-like* in YO at T0 4°C indicated by an asterisk (*) in A. All data is shown as mean±SEM and statistical differences (multiple unpaired *t*-tests, $p<0.05$) between temperatures for the respective genes are indicated by different letters. (For interpretation of the references to colour in this figure legend, the reader is referred to the web version of this article.)

The expression of the four mTOR pathway genes was influenced by temperature, but the effect differed between the organs examined. *mTOR* was significantly upregulated at high temperature in YO and in claw muscle, which also showed a similar trend for *AMPK α* and *AKT* (Fig. 6). These expression patterns contrasted with the significantly lower mRNA levels of *Rheb* and *AMPK α* in the hepatopancreas of crabs kept for two weeks at 10°C than those at 4°C, but low *Rheb* levels were also measured after the initial 4°C acclimation. The expression of the four genes showed no significant changes in ESG during the experiment.

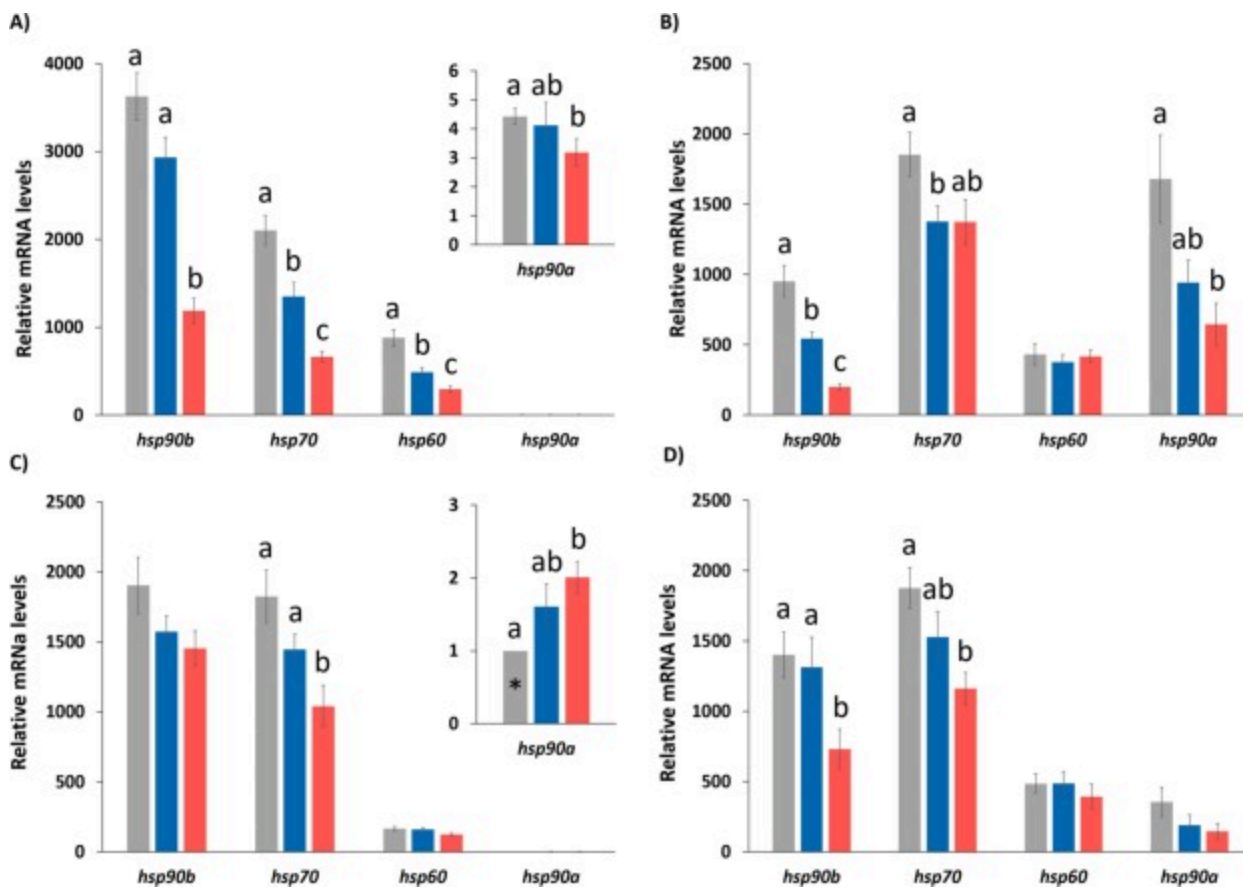


[Download: Download high-res image \(174KB\)](#)

[Download: Download full-size image](#)

Fig. 6. Tissue expression of *Rheb*, *AMPK α* , *AKT* and *mTOR* in adult red king crab after 4°C acclimation (grey) and after two additional weeks at 4°C (blue) or 10°C (red). The mRNA levels were qPCR quantified in YO, hepatopancreas, claw muscle and ESG (n=8). The results were calibrated to the mean expression of *Akt* in hepatopancreas at acclimation (*). All data is shown as mean \pm SEM and statistical differences (multiple unpaired *t*-tests, $p < 0.05$) between temperatures for the respective genes are indicated by different letters. (For interpretation of the references to colour in this figure legend, the reader is referred to the web version of this article.)

We examined the response of the adult crabs to chronic temperature changes by quantifying the expression levels of *hsp90a*, *hsp90b*, *hsp70* and *hsp60* (Fig. 7). *hsp90b* and *hsp70b* were the major transcripts in the four tissues examined, except from the high *hsp90a* levels in claw muscle. The *hsp90b*, *hsp70* and *hsp60* mRNA levels in hepatopancreas were significantly lower after two weeks at 10°C than at 4°C (Fig. 7A), and the *hsp90b* transcript showed about half the levels at high temperature also in claw muscle and YO (Fig. 7B and D). The expression of *hsp70* was also significantly downregulated in ESG at high temperature (Fig. 7C). It should be noted that the expression of the four *hsp* genes in at least one of the tissues examined was significantly higher after 4°C acclimation than after additional two weeks at 4°C or at 10°C.



[Download: Download high-res image \(228KB\)](#)

[Download: Download full-size image](#)

Fig. 7. Tissue expression of *hsp90b*, *hsp70*, *hsp60* and *hsp90a* in adult red king crab after 4°C acclimation (grey) and after two additional weeks at 4°C (blue) or 10°C (red) (n=8). The mRNA levels were qPCR quantified in A) hepatopancreas, B) claw muscle, C) ESG, D) YO. The results were calibrated to the mean expression of *hsp90a* in ESG at T0 4 °C indicated by an asterisk (*). All data is shown as mean±SEM and statistical differences (multiple unpaired *t*-tests, *p*<0.05) between temperatures for the respective genes are indicated by different letters. Note the different scaling of the y-axis in A. (For interpretation of the references to colour in this figure legend, the reader is referred to the web version of this article.)

4. Discussion

This study describes for the first time the ecdysteroid biosynthetic enzymes in anomuran crabs by *de novo* transcriptome analysis of four organs, including the YO, in red king crab. The YO shows a variety of anatomic features in crustaceans and forms an elongated structure situated on a cuticular outgrowth of the mandibles in the anomuran crab *Anapagurus hyndmanni*, while the common hermit crab (*Pagurus bernhardus*) and long-

clawed porcelain crab (*Pisidia longicornis*) have a tubular and globular YO, respectively ([Lachaise et al., 1993](#)). The crucial role played by the Halloween genes in the regulation of the molt cycle is corroborated by the well conserved sequences in red king crab, except for the Shade-like protein. Insect Shade is used by various non-decapods, such as water flea and salmon louse, for catalyzing the conversion of ecdysone to the active molting hormone 20-hydroxyecdysone (20E) ([Mykles, 2011](#); [Ventura et al., 2017](#); [Swall et al., 2021](#)), which is the main hormone also in the red king crab hemolymph ([Dvoretzky and Dvoretzky, 2010](#)). The ecdysone 20-mono-oxygenase enzyme has recently been found to be expressed by multiple *shed* genes in several decapod species, including spiny lobster and blackback land crab ([Ventura et al., 2017](#), [Ventura et al., 2018](#); [Swall et al., 2021](#)). The snow crab genome has five *shed* genes (NCBI accession PRJNA602365) of which the two *shed* transcripts identified in this study share only 50% identity. This is consistent with the relatively low homology between the *Shed* paralogs in blackback land crab ([Swall et al., 2021](#)). The presence of a Shade-like protein in red king crab suggests that Shade was retained in anomurans after the separation from brachyuran crabs ([Wolfe et al., 2019](#)), whereas brachyurans possess multiple *Shed* paralogs probably resulting from gene duplications.

King crabs (Lithodidae) are thought to have originated from the asymmetric hermit crabs (Paguridae) and later transformed to a crab-like crustacean with the pleon folded underneath the compact cephalothorax according to the so-called “hermit to king” hypothesis ([Cunningham et al., 1992](#)). The close phylogenetic relationship between lithodid and pagurid crabs is supported by the asymmetric pleon of king crabs ([Keiler et al., 2013](#)) and the high similarity of ribosomal nuclear sequence data and mitogenomes of red king crab and hermit crab, which differ considerably from the mitogenome of the anomuran squat lobster ([Kim et al., 2013](#); [Noever and Glenner, 2018](#)). Consistently, the nuclear DNA-coded protein CHH shows high similarity in red king crab and hermit crab, while they share low similarity with squat lobster CHH. The few functional analyses of crustacean CHH mutants includes the Glu54Ala substitution in mud crab CHH that did not reduce the hyperglycemic activity ([Liu et al., 2015](#)). This corresponds to one of the four substituted positions identified in anomuran CHH and suggests conserved functions, but the pleiotropic activities displayed by the brachyuran CHH ([Chen et al., 2020](#)) should be further investigated in anomurans. Earlier attempts to isolate MIH from hermit crab and squat lobster failed, but distinct CHH- and MIH-immunoreactive perikarya were localized in the hermit crab ESG ([Montagné et al., 2008](#)). In addition to these Type-I and -II peptides, respectively, red king crab also expressed the Type-III ITP-like peptide, which has been reported in several malacostracan species ([Manfrin et al., 2015](#); [Toullec et al., 2017](#)). The function of crustacean ITP-like is unknown, while a possible ecdysis-related function has been suggested for insect ITP, in addition to regulating water homeostasis ([Dircksen, 2009](#)).

Recent transcriptome analyses of the crustacean YO and ESG have revealed complex gene regulatory networks underlying the conserved signaling pathways of molting and growth (Gao et al., 2015; Das and Mykles, 2016; Oliphant et al., 2018; Shyamal et al., 2018; Su et al., 2020). The complexity seems to be increased by the influences of environmental factors, particularly temperature, on the gene expression of key regulators. Shortened molt intervals in juvenile mud crabs (*Scylla paramamosain*) at elevated temperature were associated with increased *EcR* expression (Gong et al., 2015), and temperature compensation of the expression of *MIH*, *CHH* and *mTOR* signaling genes in temperate juvenile Dungeness crabs (*Metacarcinus magister*) contributed to regulate molting in the 10°C to 20°C range (Wittmann et al., 2018). Involvement of the Halloween genes in the thermal response of crustaceans was suggested by the up- or downregulated expression of various P450 genes, including *spook*, *phantom* and *shade*, in the alligatorweed flea beetle (*Agasicles hygrophila*) acutely exposed to high temperature (Zhang et al., 2018). Red king crabs showed a tendency towards upregulation of the Halloween and *EcR* genes in the YO at elevated temperature, but large individual variations were measured that may be explained by the challenges in the dissection of the diffuse organ. These patterns of gene expression may relate to temperature-dependent acceleration of the molt cycle. In the land crab *Gecarcinus lateralis* Halloween gene and *EcR* expression increase from postmolt to intermolt and from intermolt to premolt (Benrabaa, 2019). It is likely that this is a continuous process, which could, at least in part, explain our results. The *MIH* and *CHH* mRNA levels in ESG were not affected by temperature in our study, but *MIH* was downregulated in Dungeness crab ESG at high temperature (Wittmann et al., 2018). Our results are in line with previous findings suggesting that hemolymph *MIH* and *CHH* levels are regulated on a different level of organization, i.e. protein translation and secretion (Mykles and Chang, 2020).

Tissue-specific differences became evident when high resolution analyses were employed, e.g. on KEGG enzyme level (compare Fig. 2A and B, Robalino et al., 2007), and when specific sets of genes were considered (Supplementary Table S1, Covi et al., 2010; MacLea et al., 2012; Wittmann et al., 2018). Swamp crayfish (*Procambarus clarkii*) showed tissue-specific responses to eyestalk ablation by increased *EcR* and *RXR* mRNA levels in muscle and ovaries, but downregulated receptor expression in hepatopancreas, indicating that different tissues play different roles and coordinate their functions in molting (Dai et al., 2016). Here, red king crab responded to high temperature by an upregulated trend in *EcR* expression in YO and claw muscle, while decreased *EcR* mRNA levels were found in hepatopancreas. The *mTOR* signaling genes also suggested temperature-related differences in tissue expression of which *AMPK α* and *AKT* tended to be upregulated in claw muscle at high temperature, while *AMPK α* and *Rheb* were downregulated in hepatopancreas. Tissue-specific responses to temperature were also observed in juvenile Dungeness crabs, which displayed the most

pronounced differences in cardiac expression of *Rheb* between 10°C and 15°C, with no further downregulation at exposure to 20°C after two weeks of acclimation ([Wittmann et al., 2018](#)). This indicates that protein turnover is maintained and assures the structure and function of the claw muscle and heart muscle at high temperature. Conversely, the higher expression of *Rheb* and *AMPK α* in the hepatopancreas of red king crab at 4°C compared to 10°C is consistent with the upregulation of genes involved in protein synthesis and degradation in the liver of the cold-eurythermal eelpout (*Pachycara brachycephalum*) at chronic exposure to low temperature ([Windisch et al., 2011](#)). This may reflect efficient food conversion in the cold during long-term experiments ([Siikavuopio and James, 2015](#); [Windisch et al., 2014](#)). The deep-water living adults and the shallow-water juveniles of red king crab may differ in temperature tolerance and changes in cellular energy allocation ([Stiansen et al., 2009](#); [Stoner et al., 2010](#); [Long and Daly, 2017](#)), which may relate to the expression of genes involved. Juveniles kept at either 10.5, 12.5 or 14.5°C for 20 days showed strong effects of acclimation on transcriptome level. Temperature mainly affected transcripts involved in cuticle formation and regulation, but did not affect any genes of the mTOR pathway ([Stillman et al., 2020](#)). However, changes smaller than 2-fold were excluded from their analysis, and tissue-specific responses may have equaled out in this whole organism study.

The thermal habitat of red king crab in the Barents Sea spans ambient temperatures from -0.8 to 8.5°C with males predominantly at 4–6°C and females at 5–7°C ([Pinchukov and Sundet, 2011](#)). Even though 10°C is beyond the temperature wild adult red king crabs experience, except during spawning migration, this may not be a temperature that causes cellular thermal stress affecting the folding of proteins at the time scale of our study. This may explain why the crabs exposed to 10°C for two weeks showed either lower or no changes in the expression of the four *hsp* genes examined, except for the increased *hsp90a* levels in ESG. In contrast to HSP90a, HSP90b is thought to be constitutive, but can also be induced and is probably involved in long-term cellular adaptation ([Sreedhar et al., 2004](#)). The duration and magnitude of heat stress influence the dynamics of *hsp* gene expression ([Buckley and Hofmann, 2004](#); [Logan and Buckley, 2015](#)), and the upregulation of HSPs in the eurythermal goby fish *Gillichthys mirabilis* in response to acute thermal stress was not observed after four weeks acclimation to high temperature ([Logan and Somero, 2010](#)). Downregulated *hsp* levels may also result from the faster turnover of the mRNAs than the turnover of the proteins itself ([Buckley et al., 2006](#)). Reduced mRNA levels after thermal acclimation may thus reflect the completion of the induced synthesis of the chaperones and may result in the cessation of a cellular stress response. Nevertheless, maintenance costs for homeostasis at elevated temperatures may be high and result in a trade-off between energy allocation to homeostasis and less energy available for growth

and reproduction ([Hochachka and Somero, 2002](#); [Sokolova et al., 2012](#); [Logan and Buckley, 2015](#)). The heat shock response varies among organisms that occupy different thermal environments, and contrasting with eurythermal intertidal species, such as the porcelain crab (*Petrolisthes cinctipes*), stenothermal organisms like Antarctic notothenioid fish and the gammarid crustacean *Paraceradocus gibber* do not respond to thermal stress with increased HSP synthesis ([Clark and Peck, 2009](#); [Shin et al., 2014](#); [Garland et al., 2015](#)). Intertidal snails reduced HSP protein levels at moderate temperature increase and showed elevated levels only after long-term exposure to infrequently experienced high field temperatures ([Tomanek and Somero, 1999](#), [Tomanek and Somero, 2002](#)). These studies also showed that animals exposed to constant temperatures in the laboratory exhibit lower HSP protein levels than animals sampled from the field. This resembles our observation of higher *hsp* mRNA levels in crabs sampled after acclimation at the more variable ambient temperature. The multiple temperature sensitive genes identified in juvenile red king crabs exposed to elevated temperatures comprised different clusters displaying upregulated or downregulated expression patterns dependent on the pH conditions ([Stillman et al., 2020](#)). Three contigs annotated as HSP83 only showed small and variable responses to temperature (cluster 7 in [Stillman et al., 2020](#)). While we show that constitutive and heat-inducible HSPs are expressed in a temperature-dependent and tissue-specific manner in response to acclimation, further studies should address the potential for acclimation on additional organismal levels of organization, and also the acute heat shock response in the cold-eurythermal red king crab.

5. Conclusions

Multiple expressed genes involved in various physiological functions were identified in *de novo* transcriptome assemblies from the sub-Arctic red king crab and snow crab. The phylogenetic analyses of the CHH family and Halloween genes support the phylogenetic relation between the anomuran and brachyuran crabs. Genes playing key roles in molting and growth tended to be upregulated in adult red king crab at elevated temperature, while several *hsp* genes were downregulated. The tissue- and gene-specific responses reflect regulatory processes on molecular level during acclimation of this cold-eurythermal species. The transcriptome data provides a valuable resource for comparative studies of adaptive traits, such as cold hardiness and dim light vision, in the two distant sub-Arctic crabs.

The following are the supplementary data related to this article.

 [Download: Download Word document \(810KB\)](#)

Supplementary Fig. S1. Multiple sequence alignment of the mature CHH in the anomurans red king crab, hermit crab and squat lobster together with various brachyurans. Conserved residues in one of the two groups are boxed, in addition to the dibasic cleavage site, six cysteines and C-terminal amidation site.

 [Download: Download Word document \(16KB\)](#)

Supplementary Table S1. qPCR primer sequences and amplification efficiency of the genes examined in red king crab.

 [Download: Download Word document \(17KB\)](#)

Supplementary Table S2. Halloween gene transcripts in red king crab (king) and snow crab (snow) Y-organ (YO). Contigs were either identified by text searches within the annotations and/or by blastn against *Gecarcinus lateralis* sequences ([Benrabaa, 2019](#); [Swall et al., 2021](#); [Supplementary Table S2](#)). King crab 16 and 20 were in early and late premolt, respectively, while snow crab 9 was in intermolt. KingCrab16_YO2, KingCrab16_YO3 and KingCrab20_YO1 were sampled from area #1, KingCrab20_YO2 was sampled from area #2 (see [Fig. 1B](#)). Note that it is unlikely that putative YO samples of king crab 16 were Y-organ tissue due to the absence of Halloween genes.

 [Download: Download Word document \(17KB\)](#)

Supplementary Table S3. Accession numbers of the proteins shown in [Fig. 3](#), [Fig. 4](#). Contig numbers of the *G. lateralis* genes refer to the YO and ESA transcriptomes described in [Shyamal et al. \(2018\)](#) and [Swall et al. \(2021\)](#), respectively.

 [Download: Download Word document \(21KB\)](#)

Supplementary Table S4. Functionally important gene transcripts identified in the *de novo* transcriptomes from red king crab and snow crab. Letters in raised font refer to the following transcriptomes: ^aKing16_20, ^bPreKingCrab16, ^cPostKingCrab20, ^dKingCrab20_MC, ^eKing20_YO1, ^fSnowCrab9_YOa, ^gSnow9.

Declaration of Competing Interest

The authors declare that they have no known competing financial interests or personal relationships that could have appeared to influence the work reported in this paper.

Acknowledgments

This is a contribution to the PACES II research program (WP 1.6) of the Alfred Wegener Institute, Helmholtz Center for Polar and Marine Research, funded by the Helmholtz Association, Germany. This work was partly supported by the Research Council of Norway, project no. [281053](#)).

[Recommended articles](#)

References

[Anger et al., 2003](#) K. Anger, S. Thatje, G. Lovrich, J. Calcagno

Larval and early juvenile development of *Paralomis granulosa* reared at different temperatures: tolerance of cold and food limitation in a lithodid crab from high latitudes

Mar. Ecol. Prog. Ser., 253 (2003), pp. 243-251

[Crossref ↗](#) [View in Scopus ↗](#) [Google Scholar ↗](#)

[Benrabaa, 2019](#) S.A.A.S. Benrabaa

Regulation of Halloween Genes and Ecdysteroid Responsive Genes in Molting Gland of Blackback Land Crab *Gecarcinus lateralis* by Molt-inhibiting Hormone, mTOR and TGFβ Signaling Pathways

Colorado State University, ProQuest Dissertations Publishing (2019)

(13814559)

[Google Scholar ↗](#)

[Buckley and Hofmann, 2004](#) B.A. Buckley, G.E. Hofmann

Magnitude and duration of thermal stress determine kinetics of hsp gene regulation in the goby *Gillichthys mirabilis*

Physiol. Biochem. Zool., 77 (2004), pp. 570-581

[View in Scopus ↗](#) [Google Scholar ↗](#)

[Buckley et al., 2006](#) B.A. Buckley, A.Y. Gracey, G.N. Somero

The cellular response to heat stress in the goby *Gillichthys mirabilis*: a cDNA microarray and protein-level analysis

J. Exp. Biol., 209 (2006), pp. 2660-2677

[Crossref ↗](#) [View in Scopus ↗](#) [Google Scholar ↗](#)

[Bushnell, 2015](#) B. Bushnell

BBMap Short Read Aligner, and Other Bioinformatic Tools

Available online at

<http://sourceforge.net/projects/bbmap> ↗ (2015)

[Google Scholar](#) ↗

[Cao et al., 2019](#) Q. Cao, Y. Wang, B. Chen, F. Ma, L. Hao, G. Li, C. Ouyang, L. Li

Visualization and identification of neurotransmitters in crustacean brain via multifaceted mass spectrometric approaches

ACS Chem. Neurosci., 10 (2019), pp. 1222-1229

[View article](#) [Crossref](#) ↗ [View in Scopus](#) ↗ [Google Scholar](#) ↗

[Chen et al., 2020](#) H.Y. Chen, J.Y. Toullec, C.Y. Lee

The crustacean hyperglycemic hormone superfamily: progress made in the past decade

Front. Endocrinol., 11 (2020), p. 578958

[View in Scopus](#) ↗ [Google Scholar](#) ↗

[Christiansen et al., 2015](#) J.S. Christiansen, M. Sparboe, B.S. Sæther, S.I. Siikavuopio

Thermal behaviour and the prospect spread of an invasive benthic top predator onto the Euro-Arctic shelves

Divers. Distrib., 21 (2015), pp. 1004-1013

[Crossref](#) ↗ [View in Scopus](#) ↗ [Google Scholar](#) ↗

[Chung et al., 1998](#) A.C. Chung, D.S. Durica, S.W. Clifton, B.A. Roe, P.M. Hopkins

Cloning of crustacean ecdysteroid receptor and retinoid-X receptor gene homologs and elevation of retinoid-X receptor mRNA by retinoic acid

Mol. Cell. Endocrinol., 139 (1998), pp. 209-227



[View PDF](#) [View article](#) [View in Scopus](#) ↗ [Google Scholar](#) ↗

[Chung et al., 2014](#) J.S. Chung, I.S. Ahn, O.H. Yu, D.S. Kim

Crustacean hyperglycemic hormones of two cold water crab species, *Chionoecetes opilio* and *C. japonicus*: isolation of cDNA sequences and localization of CHH neuropeptide in eyestalk ganglia

Gen. Comp. Endocrinol., 214 (2014), pp. 177-185

[Crossref](#) ↗ [Google Scholar](#) ↗

[Clark and Peck, 2009](#) M.S. Clark, L.S. Peck

HSP70 heat shock proteins and environmental stress in Antarctic marine organisms: a mini-review

Mar. Genom., 2 (2009), pp. 11-18

[View PDF](#)[View article](#)[View in Scopus ↗](#)[Google Scholar ↗](#)

[Covi et al., 2010](#) J.A. Covi, B.D. Bader, E.S. Chang, D.L. Mykles

Molt cycle regulation of protein synthesis in skeletal muscle of the blackback land crab, *Gecarcinus lateralis*, and the differential expression of a myostatin-like factor during atrophy induced by molting or unweighting

J. Exp. Biol., 213 (2010), pp. 172-183

[Crossref ↗](#)[View in Scopus ↗](#)[Google Scholar ↗](#)

[Cunningham et al., 1992](#) C.W. Cunningham, N.W. Blackstone, L.W. Buss

Evolution of king crabs from hermit crab ancestors

Nature, 355 (1992), pp. 539-542

[View in Scopus ↗](#)[Google Scholar ↗](#)

[Dai et al., 2016](#) T.H. Dai, A. Sserwadda, K. Song, Y.N. Zang, H.S. Shen

Cloning and expression of ecdysone receptor and retinoid X receptor from *Procambarus clarkii*: induction by eyestalk ablation

Int. J. Mol. Sci., 17 (2016), p. 1739

[Crossref ↗](#)[View in Scopus ↗](#)[Google Scholar ↗](#)

[Das and Mykles, 2016](#) S. Das, D.L. Mykles

A comparison of resources for the annotation of a *de novo* assembled transcriptome in the molting gland (Y-organ) of the blackback land crab, *Gecarcinus lateralis*

Integr. Comp. Biol., 56 (2016), pp. 1103-1112

[Crossref ↗](#)[View in Scopus ↗](#)[Google Scholar ↗](#)

[Das et al., 2018](#) S. Das, L. Vraspir, W. Zhou, D.S. Durica, D.L. Mykles

Transcriptomic analysis of differentially expressed genes in the molting gland (Y-organ) of the blackback land crab, *Gecarcinus lateralis*, during molt-cycle stage transitions

Comp. Biochem. Physiol., 28D (2018), pp. 37-53

[View PDF](#)[View article](#)[View in Scopus ↗](#)[Google Scholar ↗](#)

[Dawe and Colbourne, 2002](#) E.G. Dawe, E.B. Colbourne

Distribution and demography of snow crab (*Chionoecetes opilio*) males on the Newfoundland and Labrador Shelf

A.J. Paul, E.G. Dawe, E. Elnor, G.S. Jamieson, G.H. Kruse, R.S. Otto, B. Sainte-Marie, T.C. Shirley, D. Woodby (Eds.), Crabs in Cold Water Regions: Biology, Management and Economics, Alaska Sea Grant College Program, University of Alaska Fairbanks (2002), pp. 577-594

[Crossref ↗](#) [Google Scholar ↗](#)

[DeLeo et al., 2018](#) D.M. DeLeo, J.L. Pérez-Moreno, H. Vásquez-Miranda, H.D. Bracken-Grissom
RNA profile diversity across arthropoda: guidelines, methodological artifacts, and expected outcomes
Biol. Meth. Protoc., 3 (2018), Article bpy012

[View in Scopus ↗](#) [Google Scholar ↗](#)

[Dircksen, 2009](#) H. Dircksen

Insect ion transport peptides are derived from alternatively spliced genes and differentially expressed in the central and peripheral nervous system
J. Exp. Biol., 212 (2009), pp. 401-412

[Crossref ↗](#) [View in Scopus ↗](#) [Google Scholar ↗](#)

[Dvoretzky and Dvoretzky, 2010](#) A.G. Dvoretzky, V.G. Dvoretzky

Hemolymph molting hormone concentrations in red king crabs from the Barents Sea
Polar Biol., 33 (2010), pp. 1293-1298

[Crossref ↗](#) [View in Scopus ↗](#) [Google Scholar ↗](#)

[Dvoretzky and Dvoretzky, 2016](#) A.G. Dvoretzky, V.G. Dvoretzky

Inter-annual dynamics of the Barents Sea red king crab (*Paralithodes camtschaticus*) stock indices in relation to environmental factors
Polar Sci., 10 (2016), pp. 541-552

 [View PDF](#) [View article](#) [View in Scopus ↗](#) [Google Scholar ↗](#)

[Dvoretzky and Dvoretzky, 2020](#) A.G. Dvoretzky, V.G. Dvoretzky

Effects of environmental factors on the abundance, biomass, and individual weight of juvenile red king crabs in the Barents Sea
Front. Mar. Sci., 7 (2020), p. 726

[View in Scopus ↗](#) [Google Scholar ↗](#)

[Edgar, 2004](#) R.C. Edgar

MUSCLE: multiple sequence alignment with high accuracy and high throughput
Nucl. Acids Res., 32 (2004), pp. 1792-1797

[View in Scopus ↗](#) [Google Scholar ↗](#)

[Falk-Petersen et al., 2011](#) J. Falk-Petersen, P. Renaud, N. Anisimova

Establishment and ecosystem effects of the alien invasive red king crab (*Paralithodes camtschaticus*) in the Barents Sea – a review

ICES J. Mar. Sci., 68 (2011), pp. 479-488

[Crossref ↗](#) [View in Scopus ↗](#) [Google Scholar ↗](#)

[Fang et al., 2018](#) Y. Fang, L. Diao, F. Zhang, L. Ma, M. Zhao, D. Zhang, M. Sun, Y. Pi, Z. Qiao, K. Jiang

Identification of suitable reference genes of *Scylla paramamosain* for gene expression profiling in various tissues and under vibrio challenge

Crustaceana, 91 (2018), pp. 1195-1210

[Crossref ↗](#) [View in Scopus ↗](#) [Google Scholar ↗](#)

[Fanjul-Moles, 2006](#) M.L. Fanjul-Moles

Biochemical and functional aspects of crustacean hyperglycemic hormone in decapod crustaceans: review and update

Comp. Biochem. Physiol. C, 142 (2006), pp. 390-400

 [View PDF](#) [View article](#) [View in Scopus ↗](#) [Google Scholar ↗](#)

[Foyle et al., 1989](#) T. Foyle, R.K. O'Dor, R. Elner

Energetically defining the thermal limits of the snow crab

J. Exp. Biol., 145 (1989), pp. 371-393

[Crossref ↗](#) [Google Scholar ↗](#)

[Gao et al., 2015](#) Y. Gao, X. Zhang, J. Wei, X. Sun, J. Yuan, F. Li, J. Xiang

Whole transcriptome analysis provides insights into molecular mechanisms for molting in *Litopenaeus vannamei*

PLoS One, 10 (2015), Article e0144350

[Crossref ↗](#) [Google Scholar ↗](#)

[Garland et al., 2015](#) M.A. Garland, J.H. Stillman, L. Tomanek

The proteomic response of cheliped myofibril tissue in the eurythermal porcelain crab *Petrolisthes cinctipes* to heat shock following acclimation to daily temperature fluctuations

J. Exp. Biol., 2018 (2015), pp. 388-403

[Crossref ↗](#) [View in Scopus ↗](#) [Google Scholar ↗](#)

[Gong et al., 2015](#) J. Gong, K. Yu, L. Shu, H. Ye, S. Li, C. Zeng

Evaluating the effects of temperature, salinity, starvation and autotomy on molting success, molting interval and expression of ecdysone receptor in early juvenile mud crabs, *Scylla paramamosain*

J. Exp. Mar. Biol. Ecol., 464 (2015), pp. 11-17

[View PDF](#)[View article](#)[View in Scopus ↗](#)[Google Scholar ↗](#)

[Goody et al., 2014](#) R.T. Goody, L. Gramzow, P. Battlay, T. Sztal, P. Batterham, C. Robin

The molecular evolution of cytochrome P450 genes within and between *Drosophila* species

Genome Biol. Evol., 6 (2014), pp. 1118-1134

[Google Scholar ↗](#)

[Grabherr et al., 2011](#) M.G. Grabherr, B.J. Haas, M. Yassour, J.Z. Levin, D.A. Thompson, I. Amit, X.

Adiconis, L. Fan, R. Raychowdhury, Q. Zeng

Full-length transcriptome assembly from RNA-Seq data without a reference genome

Nat. Biotech., 29 (2011), p. 644

[Crossref ↗](#) [View in Scopus ↗](#) [Google Scholar ↗](#)

[Green et al., 2014](#) B.S. Green, C. Gardner, J.D. Hochmuth, A. Linnane

Environmental effects on fished lobsters and crabs

Rev. Fish Biol. Fish., 24 (2014), pp. 613-638

[Crossref ↗](#) [View in Scopus ↗](#) [Google Scholar ↗](#)

[Hall et al., 2020](#) J.R. Hall, S.J. Lehnert, E. Gonzalez, S. Kumar, J.M. Hanlon, C.J. Morris, M.L. Rise

Snow crab (*Chionoecetes opilio*) hepatopancreas transcriptome: identification and testing of candidate molecular biomarkers of seismic survey impact

Fish. Res., 234 (2020), p. 105794

[Google Scholar ↗](#)

[Hartnoll, 1982](#) R.G. Hartnoll

Growth

L.B. Ebele (Ed.), The Biology of Crustacea: Embryology, Morphology, and Genetics, 2, Academic Press, New York (1982), pp. 111-196

[Google Scholar ↗](#)

[Hartnoll, 2001](#) R.G. Hartnoll

Growth in crustacea — twenty years on

Hydrobiologia, 449 (2001), pp. 111-122

[View in Scopus ↗](#) [Google Scholar ↗](#)

[Hochachka and Somero, 2002](#) P.W. Hochachka, G. Somero

Biochemical Adaptation: Mechanisms and Process in Physiological Evolution

Oxford University Press, New York (2002)

[Google Scholar](#) ↗

[Jeon et al., 2020](#) J.H. Jeon, K.H. Moon, Y.H. Kim, Y.H. Kim

Reference gene selection for qRT-PCR analysis of season- and tissue-specific gene expression profiles in the honey bee *Apis mellifera*

Sci. Rep., 10 (2020), p. 13935

[View in Scopus](#) ↗ [Google Scholar](#) ↗

[Jones et al., 1992](#) D.T. Jones, W.R. Taylor, J.M. Thornton

The rapid generation of mutation data matrices from protein sequences

Comput. Appl. Biosci., 8 (1992), pp. 275-282

[Crossref](#) ↗ [View in Scopus](#) ↗ [Google Scholar](#) ↗

[Jørgensen and Primicerio, 2007](#) L.L. Jørgensen, R. Primicerio

Impact scenario for the invasive red king crab *Paralithodes camtschaticus* (Tilesius, 1815) (Reptantia, Lithodidae) on Norwegian, native, epibenthic prey

Hydrobiologia, 590 (2007), pp. 47-54

[Crossref](#) ↗ [View in Scopus](#) ↗ [Google Scholar](#) ↗

[Keiler et al., 2013](#) J. Keiler, S. Richter, C.S. Wirkner

Evolutionary morphology of the hemolymph vascular system in hermit and king crabs (Crustacea: Decapoda: Anomala)

J. Morphol., 274 (2013), pp. 759-778

[Crossref](#) ↗ [View in Scopus](#) ↗ [Google Scholar](#) ↗

[Kim et al., 2013](#) S. Kim, H. Choi, J. Park, G. Min

The complete mitochondrial genome of the subarctic red king crab, *Paralithodes camtschaticus* (Decapoda, Anomura)

Mitochondrial DNA, 24 (2013), pp. 350-352

[Crossref](#) ↗ [View in Scopus](#) ↗ [Google Scholar](#) ↗

[Kopylova et al., 2012](#) E. Kopylova, L. Noé, H. Touzet

SortMeRNA: fast and accurate filtering of ribosomal RNAs in metatranscriptomic data

Bioinformatics, 28 (2012), pp. 3211-3217

[Crossref](#) ↗ [View in Scopus](#) ↗ [Google Scholar](#) ↗

[Kumar et al., 2018](#) S. Kumar, G. Stecher, M. Li, C. Knyaz, K. Tamura

MEGA X: molecular evolutionary genetics analysis across computing platforms

Mol. Biol. Evol., 35 (2018), pp. 1547-1549

[View in Scopus ↗](#) [Google Scholar ↗](#)

[Lachaise et al., 1993](#) F. Lachaise, A. Le Roux, H. Hubert, R. Lafont

The molting gland of crustaceans: localization, activity, and endocrine control (a review)

J. Crust. Biol., 13 (1993), pp. 198-234

[Crossref ↗](#) [Google Scholar ↗](#)

[Le and Gascuel, 2008](#) S.Q. Le, O. Gascuel

An improved general amino acid replacement matrix

Mol. Biol. Evol., 25 (2008), pp. 1307-1320

[Crossref ↗](#) [View in Scopus ↗](#) [Google Scholar ↗](#)

[Lee et al., 2007](#) K.J. Lee, H.W. Kim, A.M. Gomez, E.S. Chang, J.A. Covi, D.L. Mykles

Molt-inhibiting hormone from the tropical land crab, *Gecarcinus lateralis*: cloning, tissue expression, and expression of biologically active recombinant peptide in yeast

Gen. Comp. Endocrinol., 150 (2007), pp. 505-513

 [View PDF](#) [View article](#) [View in Scopus ↗](#) [Google Scholar ↗](#)

[Lindquist and Mertens, 2018](#) J.A. Lindquist, P.R. Mertens

Cold shock proteins: from cellular mechanisms to pathophysiology and disease

Cell Commun. Signal., 16 (2018), p. 63

[Google Scholar ↗](#)

[Liu and Sabatini, 2020](#) G.Y. Liu, D.M. Sabatini

mTOR at the nexus of nutrition, growth, ageing and disease

Nat. Rev. Mol. Cell Biol., 21 (2020), pp. 183-203

[Crossref ↗](#) [View in Scopus ↗](#) [Google Scholar ↗](#)

[Liu et al., 2015](#) C.J. Liu, S.S. Huang, J.Y. Toullec, C.Y. Chang, Y.R. Chen, W.S. Huang, C.Y. Lee

Functional assessment of residues in the amino- and carboxyl-termini of crustacean hyperglycemic hormone (CHH) in the mud crab *Scylla olivacea* using point-mutated peptides

PLoS One, 10 (2015), Article e0134983

[Crossref ↗](#) [View in Scopus ↗](#) [Google Scholar ↗](#)

[Logan and Buckley, 2015](#) C.A. Logan, B.A. Buckley

Transcriptomic responses to environmental temperature in eurythermal and stenothermal fishes

J. Exp. Biol., 218 (2015), pp. 1915-1924

[Crossref ↗](#) [View in Scopus ↗](#) [Google Scholar ↗](#)

[Logan and Somero, 2010](#) C.A. Logan, G.N. Somero

Transcriptional responses to thermal acclimation in the eurythermal fish *Gillichthys mirabilis* (Cooper 1864)

Am. J. Physiol. Reg. Integr. Comp. Physiol., 299 (2010), pp. R843-R852

[Crossref ↗](#) [View in Scopus ↗](#) [Google Scholar ↗](#)

[Long and Daly, 2017](#) W.C. Long, B. Daly

Upper thermal tolerance in red and blue king crab: sublethal and lethal effects

Mar. Biol., 164 (2017), p. 162

[View in Scopus ↗](#) [Google Scholar ↗](#)

[Lorenzon et al., 2004](#) S. Lorenzon, P. Edomi, P.G. Giulianini, R. Mettullo, E.A. Ferrero

Variation of crustacean hyperglycemic hormone (CHH) level in the eyestalk and haemolymph of the shrimp *Palaemon elegans* following stress

J. Exp. Biol., 207 (2004), pp. 4205-4213

[View in Scopus ↗](#) [Google Scholar ↗](#)

[MacLea et al., 2012](#) K.S. MacLea, A.M. Abuhagr, N.L. Pitts, J.A. Covi, B.D. Bader, E.S. Chang, D.L. Mykles

Rheb, an activator of target of rapamycin, in the blackback land crab, *Gecarcinus lateralis*: cloning and effects of molting and unweighting on expression in skeletal muscle

J. Exp. Biol., 215 (2012), pp. 590-604

[Crossref ↗](#) [View in Scopus ↗](#) [Google Scholar ↗](#)

[Manfrin et al., 2015](#) C. Manfrin, M. Tom, G. De Moro, M. Gerdol, P.G. Giulianini, A. Pallavicini

The eyestalk transcriptome of red swamp crayfish *Procambarus clarkii*

Gene, 557 (2015), pp. 28-34



[View PDF](#) [View article](#) [View in Scopus ↗](#) [Google Scholar ↗](#)

[McCarthy et al., 2015](#) S.D. McCarthy, M.M. Dugon, A.M. Power

“Degraded” RNA profiles in Arthropoda and beyond

PeerJ, 3 (2015), Article e1436

[Crossref ↗](#) [View in Scopus ↗](#) [Google Scholar ↗](#)

[Michelsen et al., 2019](#) H.K. Michelsen, M. Sparbo, E.M. Nilssen, A.H. Kettunen, S.I. Siikavuopio, J.S. Christiansen

Thermal tolerance of invasive red king crab (*Paralithodes camtschaticus*) larvae from the Barents Sea

Shellfish Symposium “Shellfish – Resources and Invaders of the North” (2019) (Tromsø, Norway)

[Google Scholar ↗](#)

[Montagné et al., 2008](#) N. Montagné, D. Soyez, D. Gallois, C. Ollivaux, J.Y. Toullec

New insights into evolution of crustacean hyperglycaemic hormone in decapods – first characterization in Anomura

FEBS J., 275 (2008), pp. 1039-1052

[Crossref ↗](#) [View in Scopus ↗](#) [Google Scholar ↗](#)

[Moriyasu and Mallet, 1986](#) M. Moriyasu, P. Mallet

Molt stages of the snow crab *Chionoecetes opilio* by observation of morphogenesis of setae on the maxilla

J. Crust. Biol., 6 (1986), pp. 709-718

[Crossref ↗](#) [Google Scholar ↗](#)

[Mykles, 2011](#) D.L. Mykles

Ecdysteroid metabolism in crustaceans

J. Steroid Biochem. Mol. Biol., 127 (2011), pp. 196-203

 [View PDF](#) [View article](#) [View in Scopus ↗](#) [Google Scholar ↗](#)

[Mykles and Chang, 2020](#) D.L. Mykles, E.S. Chang

Hormonal control of the crustacean molting gland: Insights from transcriptomics and proteomics

Gen. Comp. Endocrinol., 294 (2020), p. 113493

 [View PDF](#) [View article](#) [View in Scopus ↗](#) [Google Scholar ↗](#)

[Noever and Glenner, 2018](#) C. Noever, H. Glenner

The origin of king crabs: hermit crab ancestry under the magnifying glass

Zool. J. Linnean Soc., 182 (2018), pp. 300-318

[Crossref ↗](#) [Google Scholar ↗](#)

[Oliphant et al., 2018](#) A. Oliphant, J.L. Alexander, M.T. Swain, S.G. Webster, D.C. Wilcockson
Transcriptomic analysis of crustacean neuropeptide signaling during the
moult cycle in the green shore crab, *Carcinus maenas*
BMC Genomics, 19 (2018), p. 711

[View in Scopus ↗](#) [Google Scholar ↗](#)

[Oug et al., 2011](#) E. Oug, S.K.J. Cochrane, J.H. Sundet, K. Norling, H.C. Nilsson
Effects of invasive red king crab, *Paralithodes camtschaticus* on soft-bottom
fauna in Varangerfjorden, northern Norway
Mar. Biodivers., 41 (2011), pp. 467-479

[Crossref ↗](#) [View in Scopus ↗](#) [Google Scholar ↗](#)

[Pfaffl, 2001](#) M.W. Pfaffl
A new mathematical model for relative quantification in real-time RT-PCR
Nucl. Acids Res., 29 (2001), Article e45

[Google Scholar ↗](#)

[Pinchukov and Sundet, 2011](#) M.A. Pinchukov, J.H. Sundet
T. Jakobsen, V.K. Ozhigin (Eds.), Red King Crab. The Barents Sea. Ecosystem, Resources,
Management. Half a Century of Russian-Norwegian Cooperation, Tapir Academic Press,
Trondheim (2011), pp. 160-166

[Google Scholar ↗](#)

[Poloczanska et al., 2016](#) E.S. Poloczanska, M.T. Burrows, C.J. Brown, J. García Molinos, B.S. Halpern,
O. Hoegh-Guldberg, C.V. Kappel, P.J. Moore, A.J. Richardson, D.S. Schoeman, W.J. Sydeman
Responses of marine organisms to climate change across oceans
Front. Mar. Sci., 3 (2016), p. 62

[View in Scopus ↗](#) [Google Scholar ↗](#)

[Pörtner, 2010](#) H.O. Pörtner
Oxygen- and capacity-limitation of thermal tolerance: a matrix for
integrating climate-related stressor effects in marine ectotherms
J. Exp. Biol., 213 (2010), pp. 881-893

[Crossref ↗](#) [View in Scopus ↗](#) [Google Scholar ↗](#)

[Pörtner and Knust, 2007](#) H.O. Pörtner, R. Knust
Climate change affects marine fishes through the oxygen limitation of
thermal tolerance
Science, 315 (2007), pp. 95-97

[Crossref ↗](#) [View in Scopus ↗](#) [Google Scholar ↗](#)

[Qu et al., 2015](#) Z. Qu, N.J. Kenny, H.M. Lam, T.F. Chan, K.H. Chu, W.G. Bendena, S.S. Tobe, J.H.L. Hui
How did arthropod sesquiterpenoids and ecdysteroids arise? Comparison of hormonal pathway genes in noninsect arthropod genomes
Genome Biol. Evol., 7 (2015), pp. 1951-1959

[View in Scopus ↗](#) [Google Scholar ↗](#)

[Quinn, 2017](#) B.K. Quinn
Threshold temperatures for performance and survival of American lobster larvae: a review of current knowledge and implications to modeling impacts of climate change
Fish. Res., 186 (2017), pp. 383-396

 [View PDF](#) [View article](#) [View in Scopus ↗](#) [Google Scholar ↗](#)

[Robalino et al., 2007](#) J. Robalino, J.S. Almeida, D. McKillen, J. Colglazier, H.F. Trent III, Y.A. Chen, M.E.T. Peck, C.L. Browdy, R.W. Chapman, G.W. Warr, P.S. Gross
Insights into the immune transcriptome of the shrimp *Litopenaeus vannamei*: tissue-specific expression profiles and transcriptomic responses to immune challenge
Physiol. Genom., 29 (2007), pp. 44-56

[Crossref ↗](#) [View in Scopus ↗](#) [Google Scholar ↗](#)

[Saxton and Sabatini, 2017](#) R.A. Saxton, D.M. Sabatini
mTOR signaling in growth, metabolism, and disease
Cell, 168 (2017), pp. 960-976

 [View PDF](#) [View article](#) [View in Scopus ↗](#) [Google Scholar ↗](#)

[Scheffers et al., 2016](#) B.R. Scheffers, *et al.*
The broad footprint of climate change from genes to biomes to people
Science, 354 (2016), Article aaf7671

[View in Scopus ↗](#) [Google Scholar ↗](#)

[Shin et al., 2014](#) S.C. Shin, D.H. Ahn, S.J. Kim, C.W. Pyo, H. Lee, M.K. Kim, J. Lee, J.E. Lee, H.W. Detrich, J.H. Postlethwait, D. Edwards, S.G. Lee, J.H. Lee, H. Park
The genome sequence of the Antarctic bullhead notothen reveals evolutionary adaptations to a cold environment
Genome Biol., 15 (2014), p. 468

[View in Scopus ↗](#) [Google Scholar ↗](#)

[Shyamal et al., 2018](#) S. Shyamal, S. Das, A. Guruacharya, D.L. Mykles, D.S. Durica
Transcriptomic analysis of crustacean molting gland (Y-organ) regulation
via the mTOR signaling pathway

Sci. Rep., 8 (2018), p. 7307

[View in Scopus ↗](#) [Google Scholar ↗](#)

[Siikavuopio and James, 2015](#) S.I. Siikavuopio, P. James
Effects of temperature on feed intake, growth and oxygen consumption in
adult male king crab *Paralithodes camtschaticus* held in captivity and fed
manufactured diets

Aquac. Res., 46 (2015), pp. 602-608

[Crossref ↗](#) [View in Scopus ↗](#) [Google Scholar ↗](#)

[Siikavuopio et al., 2017](#) S.I. Siikavuopio, R.D. Whitaker, B.-S. Sæther, P. James, B.R. Olsen, T.
Thesslund, A. Hustad, A. Mortensen
First observations of temperature tolerances of adult male snow crab
(*Chionoecetes opilio*) from the Barents Sea population and the effects on the
fisheries strategy

Mar. Biol. Res., 13 (2017), pp. 1745-1819

[Google Scholar ↗](#)

[Siikavuopio et al., 2019](#) S.I. Siikavuopio, S. Bakke, B.-S. Sæther, T. Thesslund, J.S. Christiansen
Temperature selection and final thermal preferendum of snow crab
(*Chionoecetes opilio*) from the Barents Sea

Polar Biol., 42 (2019), pp. 1911-1914

[Crossref ↗](#) [View in Scopus ↗](#) [Google Scholar ↗](#)

[Sokolova et al., 2012](#) I.M. Sokolova, M. Frederich, R. Bagwe, G. Lannig, A.A. Sukhotin
Energy homeostasis as an integrative tool for assessing limits of
environmental stress tolerance in aquatic invertebrates

Mar. Environ. Res., 79 (2012), pp. 1-15

 [View PDF](#) [View article](#) [View in Scopus ↗](#) [Google Scholar ↗](#)

[Squires, 1990](#) H.J. Squires
Decapod crustacea of the Atlantic coast of Canada

Can. Bull. Fish. Aquat. Sci, National Government Publication (1990), p. 221

[Google Scholar ↗](#)

[Sreedhar et al., 2004](#) A.S. Sreedhar, E. Kalmár, P. Csermely, Y.U. Shen

Hsp90 isoforms: functions, expression and clinical importance

FEBS Lett., 562 (2004), pp. 11-15

[View in Scopus ↗](#) [Google Scholar ↗](#)

[Stevens, 2014](#) B.G. Stevens

King Crabs on the World, Biology and Fisheries Management

CRC Press, Taylor & Francis Group (2014)

(608 pp.)

[Google Scholar ↗](#)

[Stiansen et al., 2009](#) J.E. Stiansen, O. Korneev, O. Titov, P. Arneberg

Joint Norwegian–Russian environmental status 2008

Report on the Barents Sea Ecosystem. Part II—Complete Report. IMR/PINRO Joint Report Series 2009 (2009), pp. 1-375

[Google Scholar ↗](#)

[Stillman et al., 2020](#) J.H. Stillman, S.A. Fay, S.M. Ahmad, K.M. Swiney, R.J. Foy

Transcriptomic response to decreased pH in adult, larval and juvenile red king crab, *Paralithodes camtschaticus*, and interactive effects of pH and temperature on juveniles

J. Mar. Biol. Assoc. U. K, 100 (2020), pp. 251-265

[Crossref ↗](#) [View in Scopus ↗](#) [Google Scholar ↗](#)

[Stoner et al., 2010](#) A.W. Stoner, M.L. Ottmar, L.A. Copeman

Temperature effects on the molting, growth, and lipid composition of newly-settled red king crab

J. Exp. Mar. Biol. Ecol., 393 (2010), pp. 138-147

 [View PDF](#) [View article](#) [View in Scopus ↗](#) [Google Scholar ↗](#)

[Su et al., 2020](#) S. Su, B.P. Munganga, C. Tian, J.L. Li, F. Yu, H. Li, M. Wang, X. He, Y. Tang

Analysis of Intermolt and Postmolt Transcriptomes Provides Insight Into Molecular Mechanisms of the Red Swamp Crayfish, *Procambarus clarkii* Molting

(2020), [10.1101/2020.12.09.418467 ↗](#)

[Google Scholar ↗](#)

[Swall et al., 2021](#) M.E. Swall, S.A.M. Benrabaa, N.M. Tran, T.D. Tran, T. Ventura, D.L. Mykles

Characterization of *Shed* genes encoding ecdysone 20-monooxygenase (CYP314A1) in the Y-organ of the blackback land crab, *Gecarcinus lateralis*

Gen. Comp. Endocrinol., 301 (2021), p. 113658

[View PDF](#)[View article](#)[View in Scopus ↗](#)[Google Scholar ↗](#)

[Thompson and Hawryluk, 1990](#) R.J. Thompson, M. Hawryluk

Physiological energetics of the snow crab, *Chionoecetes opilio*

Proceedings of the International Symposium on King and Tanner Crabs. Alaska Sea Grant College Program Report, AK-SG-90-04 (1990), pp. 283-291

[View in Scopus ↗](#) [Google Scholar ↗](#)

[Tomanek and Somero, 1999](#) L. Tomanek, G.N. Somero

Evolutionary and acclimation-induced variation in the heat-shock responses of congeneric marine snails (genus *Tegula*) from different thermal habitats: implications for limits of thermotolerance and biogeography

J. Exp. Biol., 202 (1999), pp. 2925-2936

[Crossref ↗](#) [View in Scopus ↗](#) [Google Scholar ↗](#)

[Tomanek and Somero, 2002](#) L. Tomanek, G.N. Somero

Interspecific- and acclimation-induced variation in levels of heat-shock proteins 70 (hsp70) and 90 (hsp90) and heat-shock transcription factor-1 (HSF1) in congeneric marine snails (genus *Tegula*): implications for regulation of *hsp* gene expression

J. Exp. Biol., 205 (2002), pp. 677-685

[Crossref ↗](#) [View in Scopus ↗](#) [Google Scholar ↗](#)

[Toullec et al., 2017](#) J.Y. Toullec, E. Corre, P. Mandon, M. Gonzalez-Aravena, C. Ollivaux, C.Y. Lee

Characterization of the neuropeptidome of a Southern Ocean decapod, the Antarctic shrimp *Chorismus antarcticus* : focusing on a new decapod ITP-like peptide belonging to the CHH peptide family

Gen. Comp. Endocrinol., 252 (2017), pp. 60-78

[View PDF](#)[View article](#)[View in Scopus ↗](#)[Google Scholar ↗](#)

[Tudge et al., 2012](#) C.C. Tudge, A. Asakura, C.T. Ah Yong

The infraorder Anomura, MacCley 1838. Chapter 70

F.R. Schram, V.C. von Vaupel Klein (Eds.), The Crustacea, Koninklijke Brill NV (2012)

[Google Scholar ↗](#)

[Vandesompele et al., 2002](#) J. Vandesompele, K. De Preter, F. Pattyn, B. Poppe, N. Van Roy, A. De Paepe, F. Spelman

Accurate normalization of real-time quantitative RT-PCR data by geometric averaging of multiple internal control genes

Genome Biol., 3 (2002), pp. 0034.1-0034.11

[Google Scholar ↗](#)

[Ventura et al., 2017](#) T. Ventura, U. Bose, Q.P. Fitzgibbon, G.G. Smith, P.N. Shaw, S.F. Cummins, A. Elizur
CYP450s analysis across spiny lobster metamorphosis identifies a long
sought missing link in crustacean development

J. Steroid Biochem. Mol. Biol., 171 (2017), pp. 262-269



[View PDF](#) [View article](#) [View in Scopus ↗](#) [Google Scholar ↗](#)

[Ventura et al., 2018](#) T. Ventura, F. Palero, G. Rotllant, Q.P. Fitzgibbon
Crustacean metamorphosis: an omics perspective

Hydrobiologia, 825 (2018), pp. 47-60

[Crossref ↗](#) [View in Scopus ↗](#) [Google Scholar ↗](#)

[Webster, 1996](#) S.G. Webster

Measurement of crustacean hyperglycaemic hormone levels in the edible
crab *Cancer pagurus* during emersion stress

J. Exp. Biol., 199 (1996), pp. 1579-1585

[Crossref ↗](#) [View in Scopus ↗](#) [Google Scholar ↗](#)

[Windisch et al., 2011](#) H.S. Windisch, R. Kathöver, H.O. Pörtner, S. Frickenhaus, M. Lucassen
Thermal acclimation in Antarctic fish: transcriptomic profiling of metabolic
pathways

Am. J. Physiol. Regul. Integr. Comp. Physiol., 301 (2011), pp. R1453-R1466

[Crossref ↗](#) [View in Scopus ↗](#) [Google Scholar ↗](#)

[Windisch et al., 2014](#) H.S. Windisch, S. Frickenhaus, U. John, R. Knust, H.O. Pörtner, M. Lucassen
Stress response or beneficial temperature acclimation: transcriptomic
signatures in Antarctic fish (*Pachycara brachycephalum*)

Mol. Ecol., 23 (2014), pp. 3469-3482

[Crossref ↗](#) [View in Scopus ↗](#) [Google Scholar ↗](#)

[Wittmann et al., 2011](#) A.C. Wittmann, D. Storch, K. Anger, H.O. Pörtner, F.J. Sartoris
Temperature-dependent activity in early life stages of the stone crab
Paralomis granulosa (Decapoda, Anomura, Lithodidae): A role for ionic and
magnesium regulation?

J. Exp. Mar. Biol. Ecol., 397 (2011), pp. 27-37



[View PDF](#) [View article](#) [View in Scopus ↗](#) [Google Scholar ↗](#)

[Wittmann et al., 2012](#) A.C. Wittmann, H.O. Pörtner, F.J. Sartoris

A role for oxygen delivery and extracellular magnesium in limiting cold tolerance of the sub-Antarctic stone crab *Paralomis granulosa*?

Physiol. Biochem. Zool., 85 (2012), pp. 285-298

[Crossref ↗](#) [View in Scopus ↗](#) [Google Scholar ↗](#)

[Wittmann et al., 2018](#) A.C. Wittmann, S.A.M. Benrabaa, D.A. López-Cerón, E.S. Chang, D.L. Mykles
Effects of temperature on juvenile Dungeness crab, *Metacarcinus magister* (Dana): survival, moulting, and mTOR signalling and neuropeptide gene expression in eyestalk ganglia, moulting gland (Y-organ), and heart
J. Exp. Biol., 221 (2018), p. 187492

[Google Scholar ↗](#)

[Wolfe et al., 2019](#) J.M. Wolfe, J.W. Breinholt, K.A. Crandall, A.R. Lemmon, E.M. Lemmon, L.E. Timm, M.E. Siddall, H.D. Bracken-Grissom
A phylogenomic framework, evolutionary timeline and genomic resources for comparative studies of decapod crustaceans
Proc. R. Soc. B, 286 (2019), p. 20190079

[Crossref ↗](#) [View in Scopus ↗](#) [Google Scholar ↗](#)

[Yamamoto et al., 2015](#) T. Yamamoto, T. Yamada, T. Kinoshita, Y. Ueda, H. Fujimoto, A. Yamasaki, K. Hamasaki
Effects of temperature on growth of juvenile snow crabs, *Chionoecetes opilio*, in the laboratory
J. Crust. Biol., 35 (2015), pp. 140-148

[Crossref ↗](#) [Google Scholar ↗](#)

[Yao et al., 1993](#) T.P. Yao, B.M. Forman, Z. Jiang, L. Cherbas, J.D. Chen, M. McKeown, P. Cherbas, R.M. Evans
Functional ecdysone receptor is the product of EcR and ultraspiracle genes
Nature, 366 (1993), pp. 476-479

[View in Scopus ↗](#) [Google Scholar ↗](#)

[Zhang et al., 2018](#) H. Zhang, M. Zhao, Y. Liu, Z. Zhou, J. Guo
Identification of cytochrome P450 monooxygenase genes and their expression in response to high temperature in the alligatorweed flea beetle *Agasicles hygrophila* (Coleoptera: Chrysomelidae)
Sci. Rep., 8 (2018), p. 17847

[View in Scopus ↗](#) [Google Scholar ↗](#)

Cited by (12)

The involvement of tumor necrosis factor receptor-associated factor 6 in regulating immune response by NF- κ B at pre-molt stage of Chinese mitten crab (*Eriocheir sinensis*)

2024, Fish and Shellfish Immunology

[Show abstract](#) ✓

Temperature-driven changes in the neuroendocrine axis of the blue crab *Callinectes sapidus* during the molt cycle

2024, General and Comparative Endocrinology

[Show abstract](#) ✓

Effects of molting on the expression of ecdysteroid responsive genes in the crustacean molting gland (Y-organ)

2024, General and Comparative Endocrinology

[Show abstract](#) ✓

Wing expansion functional analysis of ion transport peptide gene in *Sogatella furcifera* (Horváth) (Hemiptera: Delphacidae)

2024, Comparative Biochemistry and Physiology Part - B: Biochemistry and Molecular Biology

[Show abstract](#) ✓

Effects of molting on the expression of ecdysteroid biosynthesis genes in the Y-organ of the blackback land crab, *Gecarcinus lateralis*

2023, General and Comparative Endocrinology

[Show abstract](#) ✓

Acute toxic effects of diclofenac exposure on freshwater crayfish (*Procambarus clarkii*): Insights from hepatopancreatic pathology, molecular regulation and intestinal microbiota

2022, Ecotoxicology and Environmental Safety

Citation Excerpt :

...Transcriptome profiling analysis is a revolutionary and effective approach for generating reference sequence data and identifying genes or pathways involved in a variety of biological processes (Wang et al., 2009). It has been widely used in the research of aquatic crustaceans including white shrimp (*Litopenaeus vannamei*) (Chen et al., 2016), greentail prawn (*Metapenaeus bennettiae*) (Armstrong et al., 2019), red king crab (*Paralithodes camtschaticus*) (Andersen et al., 2022), snow crab (*Chionoecetes opilio*) (Andersen et al., 2022) and swimming crab (*Portunus trituberculatus*) (Fang et al., 2021) under different stresses, which can provide a powerful technology to discover novel transcripts and identify differentially expressed genes (DEGs) in the hepatopancreas of crustaceans (Rao et al., 2016; Zhang et al., 2019). Normally, intestinal microbiota can regulate many crucial physiological functions, which plays a key role in maintaining the health for the host (Zhang et al., 2020b)...

[Hide abstract](#) ^

In this study, we exposed adult male crayfish (*Procambarus clarkii*) to different concentrations of diclofenac (DCF) for 96h. In the meantime, we investigated the alternations of hepatopancreatic pathology, molecular regulation and intestinal microbiota of *P. clarkii* exposed to DCF. The results demonstrated DCF led to histological changes including epithelium vacuolization and tubule lumen dilatation in the hepatopancreas. Transcriptome sequencing analysis showed that 642 and 586 genes were differentially expressed in the hepatopancreas of *P. clarkii* exposed to 1 and 10mg/L DCF, respectively. DCF could affect the functions of antioxidation, immunity and metabolism of hepatopancreas by inducing the abnormal expressions of immune- and redox-related genes. GO enrichment results demonstrated that 10mg/L DCF exposure could modulate the processes of molting, amino sugar metabolism, protein hydrolysis and intracellular protein translocation of *P. clarkii*. Additionally, the abundances of bacterial families including Shewanellaceae, Bacteroidaceae, Vibrionaceae, Erysipelotrichaceae, Aeromonadaceae, Moraxellaceae, etc. in the intestine were significantly changed after DCF exposure, and the disruption of intestinal flora might further cause abnormal intestinal metabolism in *P. clarkii*. This study provides novel mechanistic insights into the toxic effects of anti-inflammatory drugs on aquatic crustaceans.



[View all citing articles on Scopus](#) ↗

1 These authors contributed equally to this work.



All content on this site: Copyright © 2024 Elsevier B.V., its licensors, and contributors. All rights are reserved, including those for text and data mining, AI training, and similar technologies. For all open access content, the Creative Commons licensing terms apply.

